Biogeosciences
Discussions

Wildfire history of the boreal forest of southwestern Yakutia (Siberia) over the last two millennia documented by a lake-sedimentary charcoal record

Ramesh Glückler[1,2], Ulrike Herzschuh[1,2,3], Stefan Kruse[1], Andrei Andreev[1], Stuart Andrew Vyse[1], Bettina Winkler[1,4], Boris K. Biskaborn[1], Luidmila Pestrykova[5], and Elisabeth Dietze[1]

[1]Section of Polar Terrestrial Environmental Systems, Alfred Wegener Institute Helmholtz Centre for Polar and Marine Research, Potsdam, 14473, Germany
[2]Institute for Environmental Science and Geography, University of Potsdam, Potsdam, 14476, Germany
[3]Institute for Biochemistry and Biology, University of Potsdam, Potsdam, 14476, Germany
[4]Institute of Geosciences, University of Potsdam, Potsdam, 14476, Germany
[5]Institute of Natural Sciences, North-Eastern Federal University of Yakutsk, Yakutsk, 677007, Russia

Correspondence to: Ramesh Glückler (ramesh.glueckler@awi.de) and Elisabeth Dietze (elisabeth.dietze@awi.de)

Abstract. Wildfires, as a key disturbance in forest ecosystems, are shaping the world's boreal landscapes. Changes in fire regimes are closely linked to a wide array of environmental factors, such as vegetation composition, climate change, and human activity. Arctic and boreal regions and, in particular, Siberian boreal forests are experiencing rising air and ground temperatures with the subsequent degradation of permafrost soils, leading to shifts in tree cover and species composition. Compared to the boreal zones of North America or Europe, little is known about how such environmental changes might influence long-term fire regimes in Russia. The larch-dominated eastern Siberian deciduous boreal forests differ markedly from the composition of other boreal forests, yet data about past fire regimes remain sparse. Here, we present a high-resolution macroscopic charcoal record from lacustrine sediments of Lake Khamra (SW Yakutia, Siberia) spanning the last c. 2200 years, including information about charcoal particle sizes and morphotypes. Our results reveal a phase of increased charcoal accumulation between 600–900 CE, indicative of relatively high amounts of burnt biomass and high fire frequencies. This is followed by an almost 900-year-long period of low charcoal accumulation without significant peaks, likely corresponding to cooler climate conditions. After 1750 CE fire frequencies and the relative amount of biomass burnt start to increase again, coinciding with a warming climate and increased anthropogenic land development after Russian colonisation. In the 20th century, total charcoal accumulation decreases again to very low levels, despite higher fire frequency, potentially reflecting a change in fire management strategies and/or a shift of the fire regime towards more frequent, but smaller fires. A similar pattern for different charcoal morphotypes and comparison to a pollen and non-pollen palynomorph record from the same sediment core indicate that broad-scale changes in vegetation

composition were probably not a major driver of recorded fire regime changes. Instead, the fire regime of the last two millennia at Lake Khamra seems to be controlled mainly by a combination of short-term climate variability and anthropogenic fire ignition and suppression.

1 Introduction

35   Wildfires in Siberia have become larger and more frequent in recent years (Walker et al., 2019), drawing attention from both scientists and the wider public. The occurrence of wildfires in high latitudes is closely linked to a dry climate and to rising temperatures, which have been increasing at more than twice the rate of elsewhere (Jansen et al., 2020; Lenton, 2012). With ongoing warming, the established fire regimes will likely be subject to future change. Fire has long been the most important ecological disturbance in boreal forests, shaping the appearance and

40   composition of the world's largest terrestrial biome (Goldammer and Furyaev, 1996). It acts as a main driver behind the boreal forest's carbon pool, which comprises a third of all globally stored terrestrial carbon (Kuuluvainen and Gauthier, 2018) and strikes a fine balance between emitting carbon during combustion and sequestering it during following regrowth (Alexander et al., 2012; Ito, 2005; Köster et al., 2018). Wildfires are thought to turn this balance towards acting as a net source of emissions (Walker et al., 2019), while posing

45   increasing risks to human livelihoods and infrastructure (Flannigan et al., 2009). Additionally, fire in boreal forests may trigger tipping points in tree mortality, tree density, and shifts in vegetation composition with continued global warming (Herzschuh, 2020; Lenton et al., 2008; Scheffer et al., 2012; Wang and Hausfather, 2020). For these reasons, a prediction of potential future changes in boreal fire regimes is imperative to eventually inform and prepare adapted fire management strategies in a warming arctic and subarctic boreal. However, data about long-

50   term changes in fire regimes, a prerequisite for model validation, are still very sparse for large parts of the Russian boreal, despite it comprising more than half of the world's coniferous tree stocks (Nilsson and Shvidenko, 1998). Macroscopic charcoal particles in sediment archives, derived from biomass burning, are commonly used as a proxy for fire activity (e.g. Clark, 1988; Conedera et al., 2009; Remy et al., 2018; Whitlock and Larsen, 2001). Charcoal records are an important tool for tracking past changes in fire regimes and searching for underlying causes and

55   effects, from local to global scales (Marlon et al., 2008, 2013; Power et al., 2008). In recent years the evaluation of charcoal particle distributions was expanded to infer past fire frequencies (Higuera et al., 2007) and estimate source areas (Duffin et al., 2008; Leys et al., 2015), the type of vegetation burning with charcoal morphotypes (Enache and Cumming, 2007; Feurdean et al., 2020; Mustaphi and Pisaric, 2014), and fire intensity with charcoal reflectance (Hudspith et al., 2015). Yet, the Global Paleofire Database (www.paleofire.org; Power et al., 2010)

60   lists only a few continuously sampled macroscopic charcoal records across the Siberian boreal forest. Only recently
have charcoal records of sufficient temporal resolution allowed the assessment of fire return intervals in western
Siberian evergreen forests and they reveal close fire–vegetation relationships (Barhoumi et al., 2019; Feurdean et
al., 2020). More studies have been conducted in North America (e.g. Frégeau et al., 2015; Hély et al., 2010;
Hoecker et al., 2020; Waito et al., 2018) and boreal Europe (e.g. Aakala et al., 2018; Feurdean et al., 2017; Molinari

65   et al., 2020; Wallenius, 2011). However, comparisons across boreal study sites are complicated by the differing
predominant fire regimes in North America (high-intensity crown fires) and Eurasia (lower-intensity surface fires)
(de Groot et al., 2013).

The main fire regimes in the European and western Siberian evergreen boreal forest also differ markedly from
those of its larch-dominated, deciduous counterpart in eastern Siberia. Many prevalent evergreen conifers (*Pinus*

70   *sibirica*, *Picea obovata*, *Abies sibirica*) are commonly seen as fire avoiders and are more susceptible to crown fires
(Dietze et al., 2020; Isaev et al., 2010; Rogers et al., 2015). The predominant eastern Siberian larches (*Larix
gmelinii*, *L. cajanderi*, *L. sibirica*), on the other hand, can resist fires with an insulating bark protecting the
cambium from heat, while their deciduous and self-pruning nature restricts fires from reaching the crown (Wirth,
2005). Moreover, larches are thought to benefit from occasional surface fires, leading to more saplings by clearing

75   the lower vegetation layers of plant litter and mosses, although this might become a risk for young trees if fire
frequencies increase above a certain threshold (Sofronov and Volokitina, 2010). Surface fires in larch forest might
also play a role in the long-term preservation of permafrost (Dietze et al., 2020; Herzschuh, 2020; Herzschuh et
al., 2016). These different fire strategies within the Siberian boreal forest reinforce the need for fire reconstructions
towards the eastern part to evaluate changes in fire regimes depending on the prevalent tree species and to obtain

80   a biome-specific overview of fire regimes throughout time.

The main goal of this study is to start filling a pronounced gap in the global distribution of macroscopic charcoal
records by providing the first continuously sampled, high-resolution macroscopic charcoal record from eastern
Siberia, using charcoal size classes and morphotypes. We specifically aim to answer the following research
questions: (I) How did the fire regime in south-west Yakutia change throughout the last two millennia? (II) How

85   might reconstructed fire history relate to common drivers behind changes in fire regimes (climate, vegetation,
humans)?

2 Study site and methods

2.1 Location

Lake Khamra (59.97 °N, 112.96 °E) is located c. 30 km north-west of the Lena River in south-west Yakutia
90   (Republic of Sakha, Lensky District), at an elevation of 340 m a.s.l. (Fig. 1a). Covering an area of 4.6 km² the lake
has a maximum water depth of 22.3 m. The catchment area of 107.4 km² stretches around the gentle slopes
surrounding the lake and extends in a south-western direction along the main inflow stream. It is embedded in a
region of Cambrian bedrock made up of dolomite and limestone with transitions to silty Ordovician sandstone and
locally restricted areas of clayey Silurian limestone (Chelnokova et al., 1988).

95   The surroundings of the lake were unglaciated during the Last Glacial Maximum (LGM; Ehlers and Gibbard,
2007) and discontinuous or sporadic permafrost can be present within the study area (Fedorov et al., 2018).
Morphological features suggest that Lake Khamra is an intermontane basin lake that is not of thermokarst origin,
because of a lack of steep slopes (Katamura et al., 2009a), a maximum lake depth of 22.3 m compared to
thermokarst lakes reaching mostly <10 m (Bouchard et al., 2016; West and Plug, 2008), and the absence of
100   cryogenic features such as ice wedges indicating thermokarst processes (Katamura et al., 2009b; Séjourné et al.,
2015). Accordingly, the regional soil volumetric ice content as broadly defined by Fedorov et al. (2018) is probably
below the 30% required for the development of thermokarst lakes (Grosse et al., 2013).

The region lies within the transition zone of evergreen to deciduous boreal forest. The lake catchment is covered
by dense mixed-coniferous forest consisting of *Larix gmelinii* with *Pinus sylvestris, P. sibirica*, *Picea obovata*,
105   *Abies sibirica*, *Betula pendula,* and *Salix* sp. (Kruse et al., 2019).

The continental climate of southern Yakutia is characterised by a short, mild growing season and extremely cold
winters. The mean temperature of July at c. 18°C is contrasted by the low mean temperature in January of about -
40°C (Fedorov et al., 2018). Mean annual precipitation from 2000–2016 at the closest weather station in Vitim (c.
60 km south-west of Lake Khamra) was c. 480 mm, with highest values in July to September (Russian Institute of
110   Hydrometeorological Information, 2020).

The regional climate is mainly controlled by the large-scale Arctic Oscillation (AO) pattern emerging between
cold high-latitude and mild mid-latitude air masses (Wu and Wang, 2002). It has been suggested that positive
phases of AO, with low atmospheric pressure over the Arctic directing warm air from the south, potentially
increase Siberian fire activity (Balzter et al., 2005; Kim et al., 2020).

115   Overall population density of the Lensky District is rather low at 0.5 inhabitants per km² (Administrative Center
Lensk, 2015). Lake Khamra is c. 40 km north of one of the larger district settlements, Peleduy, with a population

of c. 5000 inhabitants. Traces of logging activity are visible on satellite imagery c. 10 km from the lake, while in its direct vicinity only winter forest tracks are kept open. We discovered traces of recent wildfire disturbance at vegetation plots around the lake, i.e. trees with fire scars on their trunk or burnt bark. These traces likely correspond

120   to recent fires within the catchment in 2007 and 2014 as captured by the remotely sensed forest loss data of Hansen et al. (2013) (Fig. 1b, c).
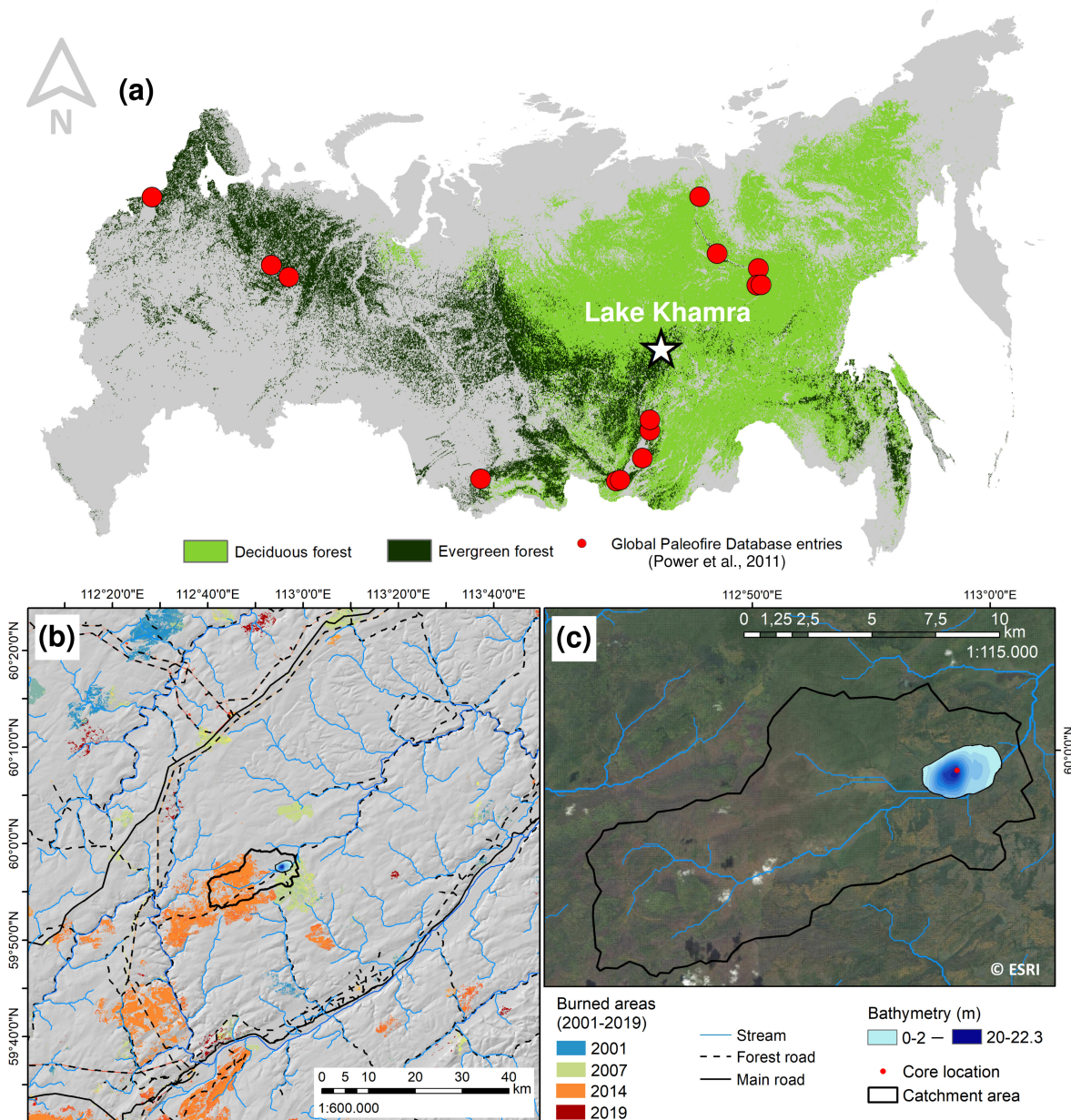
Figure 1: (a) Position of Lake Khamra and existing Global Paleofire Database entries (accessed October 6, 2020) within the deciduous and evergreen boreal forests of Russia (land cover classification based on © ESA Climate Change Initiative Land cover project, provided via the Centre for Environmental Data Archival (CEDA). (b) Infrastructure and burned areas between 2001–2019 CE (Hansen et al., 2013) in the vicinity of the lake (centre). (c) Lake Khamra with bathymetry and catchment area/watershed (black line) (Service layer credits: Esri, DigitalGlobe, GeoEye, i-cubed, USDA, USGS, AEX, Getmapping, Aerogrid, IGN, IGP, swisstopo, and the GIS User Community).

6

Biogeosciences
Discussions

Open Access

EGU

2.2 Fieldwork and subsampling

130 Fieldwork at Lake Khamra was conducted in August 2018. The 242-cm-long sediment core EN18232-3 was obtained using a hammer-modified UWITEC gravity corer at the deepest part of the lake (22.3 m), based on water depth measurements using a surveying rope and a hand-held HONDEX PS-7 LCD digital sounder. From the same location, a parallel short sediment core (EN18232-2, 39 cm length) was retrieved and subsampled in the field at increments of 0.5 cm (upper 20 cm) and 1 cm (lower 19 cm) for lead-210 and caesium-137 (Pb/Cs) age dating.

135 The sediment core, stored in a plastic tube, and all sediment samples, kept in Whirl-Pak bags, were shipped to the Alfred Wegener Institute, Helmholtz Centre for Polar and Marine Research (AWI) in Potsdam and placed in storage at 4°C. In October 2018, sediment core EN18232-3 was opened and cut in half in a cooled room under sterile conditions. While one half was archived, the other half was subsampled for proxy analysis and radiocarbon (^{14}C) dating. The sampling scheme included one 2 mL sample from the midpoint of every 2 cm increment (n =

140 120), used for the combined palynological analysis and charcoal extraction, and two c. 1 mL samples between each pair of larger samples (n = 234), used specifically for charcoal extraction to ensure a continuous record of charcoal concentration. Bulk sediment samples for ^{14}C age dating were extracted every 20 cm (n = 12). At 85.5 cm core depth, a c. 2 cm long piece of wood was removed from the sediment core for ^{14}C dating. Due to a lack of any other larger organic structures, more macrofossil samples were picked while wet-sieving bulk sediment

145 samples (n = 15). Except for one case, a clear determination of their origin was not possible because of the small size of these samples.

2.3 Laboratory analyses

2.3.1 Lithology and age dating

Sediment core EN18232-3 was visually described before sampling. Water content and bulk density were

150 determined in subsamples from 120 sampling increments every 2 cm.

To establish a chronology, all bulk and macrofossil samples were sent to AWI Bremerhaven for ^{14}C age dating at the MICADAS (Mini Carbon Dating System) laboratory. Subsamples of the parallel short core EN18232-2 (n = 19) were sent to the University of Liverpool Environmental Radioactivity Laboratory for Pb/Cs age dating, analysing ^{210}Pb, ^{226}Ra, ^{137}Cs, and ^{241}Am by direct gamma assay with Ortec HPGe GWL series well-type coaxial

155 low background intrinsic germanium detectors (Appleby et al., 1986). After careful evaluation of age dating results, an age-depth model was computed using Bacon v.2.4.3 (Blaauw and Christen, 2011; package "rbacon";

Blaauw et al., 2020), combining Pb/Cs and adjusted ^{14}C ages of all bulk samples calibrated with the IntCal20 ^{14}C calibration curve (Reimer et al., 2020).

2.3.2 Macroscopic charcoal

160   We developed a sample preparation protocol that allows for the extraction of both macroscopic charcoal and the smaller pollen fraction including non-pollen palynomorphs (NPP) from the same sediment sample. *Lycopodium* tablets (Department of Geology, Lund University), used as marker grains in the palynological analysis, were dissolved in 10% HCl and added to the sediment samples. These were subsequently wet-sieved at 150 µm mesh width for separation of the macroscopic charcoal from smaller fractions (e.g. Conedera et al., 2009; Dietze et al.,

165   2019; Hawthorne et al., 2018). The suspension with the <150 µm-fraction was collected in a bowl below the sieve. This "pollen subsample" was then iteratively added to a falcon tube, centrifuged, and decanted prior to further preparation for palynological analysis. The >150 µm fraction in the sieve was rinsed together under a gentle stream of tap water before being transferred into another falcon tube. This macroscopic "charcoal subsample" was then left to soak overnight in c. 15 mL of bleach (<5% NaClO) to minimise the potential counting error from darker,

170   non-charcoal organic particles (Halsall et al., 2018; Hawthorne et al., 2018).

Counting of 304 charcoal samples was done under a reflected-light stereomicroscope at 10–40x magnification. All particles that appeared opaque and mostly jet-black with charred structures were counted in every given sample (see Brunelle and Anderson, 2003; Hawthorne et al., 2018). In addition, counted particles were grouped into three size classes (150–300 µm, 300–500 µm, and >500 µm measured along a particle's longest axis; Dietze et al., 2019)

175   and after similarities in shape (charcoal morphotypes; Enache and Cumming, 2007). For size reference, preparatory needles with known diameters of 300 and 500 µm were used that could be placed next to a charcoal particle. These needles also allowed the evaluation of the flexibility of particles of uncertain origin, since charcoal fragments are described as fragile and non-bendable (Whitlock and Larsen, 2001).

Grouping of particles after their shape was based on the morphotype classification scheme by Enache and

180   Cumming (2007) and extended by three additional types to represent the variety of charcoal particles found at the study site. The original scheme differentiates between irregular (types M, P), angular (types S, B, C), and elongated (types D, F) shapes and further divides those depending on whether they show a visible structure or ramifications. The three added types appear as highly irregular particles (type X), elongated, fibrous particles (type E), and slightly charred, partially transparent particles (type Z), the latter of which are not included in the total charcoal

185   sum. For correlations and visualisations, the morphotypes were grouped in their respective main categories (irregular, angular, or elongated). Within the topmost c. 50 cm of the sediment core, relative morphotype

distributions were retrospectively derived from counts of 67 subsamples. At that time, 11 samples had already been used for other purposes and thus lack information on morphotype classification.

Eight randomly selected samples were counted a second time to obtain an estimate of counting uncertainty and
190 ambiguity in charcoal identification.

2.3.3 Palynological samples

Established protocols following Andreev et al. (2012) were applied to the "pollen subsample" (n = 35). Of these samples, 11 were chosen specifically from intervals with high charcoal concentrations, whereas the others were spread across the sediment core. Samples were treated with boiling potassium hydroxide for 10 min, sieved and
195 left to soak in 18 mL hydrofluoric acid (40% HF) overnight. After two additional treatments with hot HF (1.5 h each), acetolysis was performed using acetic acid and in a second step a mixture of acetic anhydrite and sulfuric acid. After being fine-sieved in an ultrasonic bath, the samples were suspended in glycerol.

Pollen and NPPs were counted together with the added *Lycopodium* spores on pollen slides under a transmitting light microscope, with a minimum count sum of 300 particles. For subsequent analyses, pollen and spore amounts
200 relative to the respective total counts were used.

2.4 Statistical methods

Statistical analysis was carried out in R v.4.0.2 (R Core Team, 2020). To asses fire history, two different approaches were applied that decompose the charcoal record into a background component, representing long-term variations in charcoal accumulation and particle taphonomy, and a peak component, representing
205 predominantly local charcoal accumulation during fire episodes (Higuera et al., 2007, 2009; Kelly et al., 2011). First, we used the well-established "CharAnalysis" method (Higuera et al., 2009; R script by Dietze et al., 2019), referred to as "classic CHAR". We interpolated the charcoal record to equally spaced time intervals according to its median resolution and calculated the charcoal accumulation rate (CHAR, particles cm^{-2} yr^{-1}; package "paleofire" v.1.2.4, function "pretreatment"; Blarquez et al., 2014). A background component was determined by computing
210 a locally estimated scatterplot smoothing (LOESS) at a window width of 25% of the total record length (package "locfit" v.1.5-9.4, function "locfit"; Loader et al., 2020). This window width was found to result in an efficient distribution of a signal-to-noise index (SNI) >3 after Kelly et al. (2011), which indicates a high degree of separation between signal and noise (Barhoumi et al., 2019; Kelly et al., 2011). A peak component was created by subtracting the background component from the timeseries. By fitting two Gaussian distributions into the histogram of the
215 peak component (package "mixtools" v.1.2.0, function "normalmixEM"; Benaglia et al., 2009), a global threshold

was defined at the 99th percentile of the noise distribution (Whitlock and Anderson, 2003). All peak component values exceeding the threshold were subsequently identified as signal (representing fire episodes) and marked when they overlapped with periods of SNI >3. Longer window widths in the statistical analysis of classic CHAR would have resulted in more fire episodes (up to 100%) above the proposed cutoff-value of SNI = 3 (Kelly et al.,

220 2011), but also in a strong averaging of the record. With all of the few fire episodes at SNI <3 lying very close to the cut-off value, this was seen as a reason to include them in the estimation of fire return intervals (FRIs).

FRIs were determined as the temporal difference between subsequent fire episodes. An illustration of fire frequency was derived by counting all identified fire episodes within a moving window spanning 200 yrs before applying a LOESS of the same window width to provide a clearer visualisation.

225 To account for accumulated uncertainties from both the chronology and the counting procedure, we used a Monte Carlo (MC) based approach (for detailed description and R script see Dietze et al., 2019), referred to as "robust CHAR". In short, it describes both the age and proxy values of each sample as Gaussian distributions, creating a pool from which random values are sampled. As inputs we used the 2σ range of Pb/Cs ages and 1σ range of calibrated and adjusted ^{14}C ages to scale the general magnitudes of uncertainty between the two dating methods to

230 comparable dimensions. For proxy uncertainty, the average deviation between the repeatedly counted samples was used (c. 20%). Five thousand MC runs were performed and output data resolution set at three times the record's median temporal resolution (18 yrs). Robust CHAR was then divided into background and peak components, similarly to classic CHAR, but by computing 1000 randomly sampled LOESS fits at varying window widths ranging from 5–25% of the record length, thereby not relying on an individual user-input value (Blarquez et al.,

235 2013).

The statistical approach outlined above (classic and robust CHAR including the determination of SNI, FRIs, and fire frequency) was also applied to the charcoal size classes and morphotype categories, respectively (see Supplement).

A principal component analysis (PCA; package "stats"; R Core Team, 2020) was used to assess relationships

240 among the various centred log-ratio (clr) transformed (package "compositions"; van den Boogaart et al., 2020) relative distributions of charcoal particle classes. To evaluate potential associations between charcoal accumulation and vegetation we applied correlation tests using Kendall's τ (package "psych"; Revelle, 2020) to clr-transformed relative distributions of pollen types and charcoal classes following Dietze et al. (2020).

3. Results

245 **3.1 Lithological sediment properties and chronology**

Sediment core EN18232-3 shows no lamination or visible changes in its brown colour or the texture of the sediment matrix. Its homogenous appearance is underlined by both uniform mean dry bulk density (184 ± 4 mg cm⁻³, mean ± 1σ) and water content (83 ± 4%).

Only 9 of the 15 macrofossil samples were large enough in size to be used for ^{14}C dating, although mostly only

250 slightly above the minimum amount of carbon (Table 1a). As Pb/Cs dating from the parallel short core EN18232-2 reveals no disturbances in its uniform sedimentation rate, the ages are expected to be applicable to the main core EN18232-3 from the same location within the lake and thus can be compared to the respective ^{14}C ages. Noticeably, the topmost ^{14}C bulk sample dates to 1415 ± 27 ^{14}C yrs BP (before present, i.e. before 1950 CE), whereas the Pb/Cs method from the parallel core confirms the expected recent surface age (Table 1b). This ^{14}C age offset can

255 have a variety of causes, such as sediment mixing processes (Biskaborn et al., 2012), the presence of old organic carbon (Colman et al., 1996; Vyse et al., 2020), or dissolved carbonate rock (hard-water effect; Keaveney and Reimer, 2012; Philippsen, 2013).

In the case of Lake Khamra, located in a zone of discontinuous permafrost and bedrock containing early Palaeozoic carbonates, the observed ^{14}C age offset is a likely consequence of input of both old organic and inorganic carbon

260 through the south-western inflow stream. The magnitude of this offset is documented by the difference between the ^{14}C bulk surface sample and the corresponding Pb/Cs age, which shows a recent surface age and is not affected by "old carbon" input. Furthermore, multiple indicators support the assumption that accumulation of old carbon not only happened recently, but rather constitutes an ongoing process in this lake system: (I) Treating the surface ^{14}C age as an outlier without also adjusting the other ^{14}C dates would necessarily lead to a strong shift in

265 sedimentation rates, which is neither reflected by the homogenous appearance and density, nor the uniform sedimentation rate as implied by the Pb/Cs method. (II) Macrofossil ^{14}C ages provide direct evidence for the influence of old carbon on bulk samples at various depths (e.g. macrofossil age of 9902 ± 97 ^{14}C yrs BP in a sediment matrix that dates back to only c. 100 yrs BP according to the parallel core's unaffected Pb/Cs method at depth 21–22 cm).

270 For these reasons, the documented age offset (mean ± 1σ) in the topmost ^{14}C sample was used to adjust all other ^{14}C bulk samples (Colman et al., 1996; Vyse et al., 2020). Although macrofossil samples are usually thought to be superior in precision to bulk sediment for age dating purposes (Hajdas et al., 1995; Wohlfarth et al., 1998), within

the present environment we cannot exclude a potential permafrost origin as well as measurement uncertainties due to their small size. For this reason, they were not used for constructing the chronology.

275   The age-depth model created according to these observations (Fig. 2) shows a smooth transition from Pb/Cs dates towards adjusted bulk ^{14}C ages. Its uniform sedimentation rate mirrors the sediment core's homogenous composition and supports the underlying assumption of a rather constant magnitude of old carbon influence on bulk ^{14}C ages. Based on this chronology, the sediment core spans c. 2350 years across its 242 cm length. The continuously sampled charcoal record spans c. 2160 years and thus reaches back from 2018 CE until c. 140 BCE.

280

Depth (cm)	Type	F^{14}C ± 1σ	^{14}C BP ± 1σ	cal BP ± 2σ	cal BP ± 2σ (adjusted)	Comment
0.5*	**Bulk**	**0.8385 ± 0.0029**	**1415 ± 27**	**1321.5 ± 32.5**	**-**	**^{14}C age-offset**
20–21	Macrofossil	0.8876 ± 0.0119	958 ± 108	924.5 ± 247.5	-	Unknown source, 18 µg C
21–22	Macrofossil	0.2915 ± 0.0035	9902 ± 97	11459 ± 277	-	Unknown source, 127 µg C
25–26	Macrofossil	0.7669 ± 0.0072	2132 ± 75	2132.5 ± 191.5	-	Unknown source, 144 µg C
29–31	Macrofossil	0.9069 ± 0.0081	785 ± 72	733 ± 170	-	Birch seed, 32 µg C
30–31	Macrofossil	0.9473 ± 0.0090	435 ± 76	466 ± 156	-	Unknown source, 36 µg C
35–37*	**Bulk**	**0.8054 ± 0.0028**	**1738 ± 28**	**1639 ± 70**	**385 ± 79**	
49–50	Macrofossil	0.7719 ± 0.0077	2080 ± 80	2069 ± 237	-	Unknown source, 56 µg C
49–51	Macrofossil	0.7720 ± 0.0098	2079 ± 102	2077 ± 254	-	Unknown source, 22 µg C
77–79*	**Bulk**	**0.7287 ± 0.0030**	**2542 ± 33**	**2622 ± 127**	**1067 ± 106**	
85.5	Macrofossil	0.8566 ± 0.0031	1244 ± 29	1172 ± 100	-	Piece of wood, 986 µg C
97–99	Macrofossil	0.7799 ± 0.0074	1997 ± 76	1930 ± 191	-	Unknown source, 35 µg C
117–119*	**Bulk**	**0.7164 ± 0.0025**	**2679 ± 28**	**2797.5 ± 46.5**	**1187 ± 96**	
157–159*	**Bulk**	**0.6773 ± 0.0027**	**3130 ± 32**	**3345.5 ± 97.5**	**1628.5 ± 72.5**	
197–199*	**Bulk**	**0.6417 ± 0.0026**	**3564 ± 32**	**3847.5 ± 121.5**	**2156 ± 148**	
237–239*	**Bulk**	**0.6427 ± 0.0023**	**3551 ± 28**	**3822 ± 99**	**2152.5 ± 146.5**	

Table 1a: ^{14}C age dating results of bulk and macrofossil samples from core EN18232-3. All samples used for the creation of the chronology are marked with a * in the first column.

Depth (cm)	^{210}Pb (total, Bq kg^{-1})	^{210}Pb ± 1σ (unsupported, Bq kg^{-1})	^{137}Cs ± 1σ (Bq kg^{-1})	Age BP ± 1σ	Year CE ± 1σ
0	-	-	-	-68 ± 0	2018 ± 0
0.5–1	1707.8 ± 38.5	1664.7 ± 38.9	38.7 ± 4.1	-64 ± 0	2014 ± 0
1.5–2	1382.2 ± 33.3	1340.7 ± 33.8	43.4 ± 4.3	-58 ± 1	2008 ± 1
2.5–3	1096.4 ± 32.4	1046.9 ± 32.8	54.0 ± 3.7	-52 ± 1	2002 ± 1
3.5–4	817.8 ± 24.7	780.6 ± 25.0	61.9 ± 3.8	-46 ± 2	1996 ± 2
4.5–5	507.4 ± 18.6	476.8 ± 18.9	106.7 ± 3.5	-39 ± 2	1989 ± 2
5.5–6	505.2 ± 22.5	467.4 ± 22.9	118.7 ± 4.9	-33 ± 3	1983 ± 3
6.5–7	464.8 ± 14.6	427.2 ± 14.9	144.7 ± 3.3	-26 ± 4	1976 ± 4
7.5–8	316.2 ± 19.3	284.6 ± 19.6	216.8 ± 5.6	-20 ± 4	1970 ± 4
8.5–9	262.8 ± 14.6	222.6 ± 15.0	286.1 ± 4.6	-13 ± 5	1963 ± 5
9.5–10	254.6 ± 11.5	216.1 ± 11.8	136.2 ± 3.2	-6 ± 5	1956 ± 5
10.5–11	254.8 ± 14.7	220.6 ± 14.9	47.8 ± 2.6	1 ± 5	1949 ± 5
11.5–12	152.7 ± 13.8	114.8 ± 14.2	19.4 ± 2.6	8 ± 5	1942 ± 5
12.5–13	148.0 ± 9.8	106.0 ± 10.0	12.7 ± 1.3	16 ± 6	1934 ± 6
13.5–14	110.5 ± 7.0	73.7 ± 7.2	9.6 ± 1.3	23 ± 7	1927 ± 7
14.5–15	89.1 ± 7.7	57.8 ± 7.9	5.2 ± 0.9	31 ± 8	1919 ± 8
16–17	81.7 ± 8.8	45.7 ± 9.1	2.2 ± 1.4	45 ± 10	1905 ± 10
18–19	68.6 ± 9.7	26.0 ± 10.0	2.0 ± 1.4	61 ± 13	1889 ± 13
20–21	47.8 ± 6.4	11.9 ± 6.6	1.0 ± 1.0	78 ± 16	1872 ± 16
22–23	47.3 ± 7.6	8.2 ± 7.9	1.8 ± 1.1	95 ± 19	1855 ± 19

285 **Table 1b: Pb/Cs age dating results from parallel short core EN18232-2 (analysed by P. Appleby, pers. communication, 2019)**
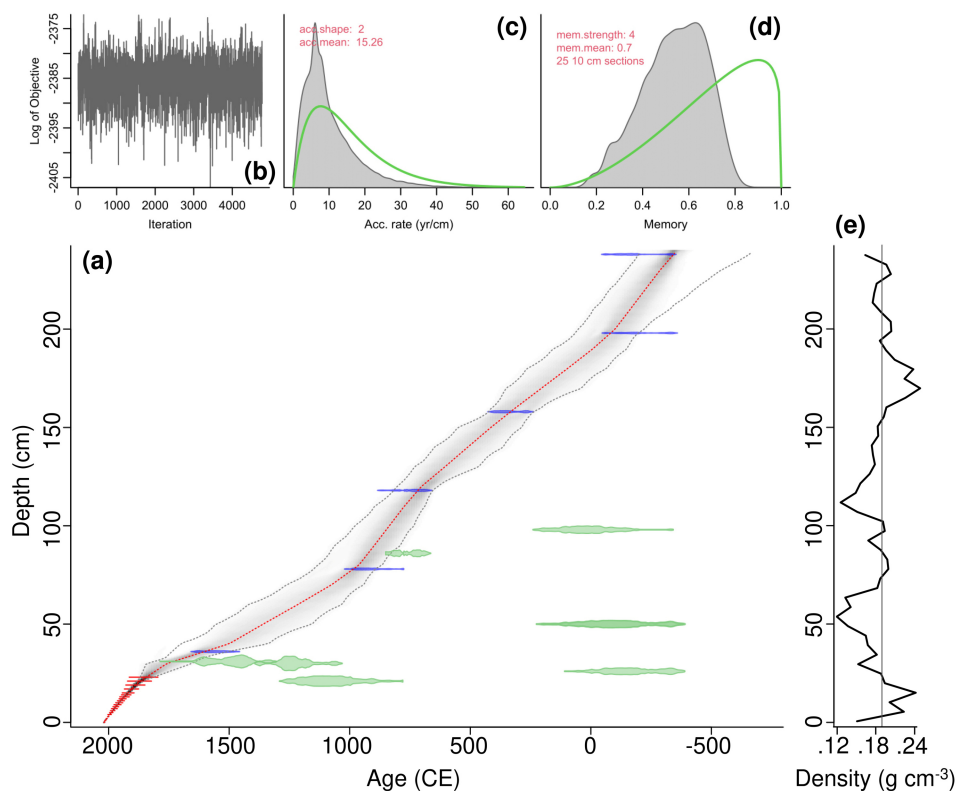
Figure 2: (a) Bayesian age-depth model applying Bacon (Blaauw and Christen, 2011) to several types of determined
290 **sediment ages (red = Pb/Cs, blue = ^{14}C bulk sediment, green = ^{14}C macrofossils, grey lines = 2σ range, red line = median).**
(b) Model iteration log. (c), (d) Prior (green line) and posterior (grey area) distributions for accumulation rate and
memory, respectively. (e) Dry bulk density of sediment core EN18232-3 (grey line = mean).

3.2 Reconstructed fire regime

The median temporal resolution of the charcoal record is 6 yrs and its samples contain 8.1 ± 5.1 (mean ± 1σ)
295 charcoal particles per cm³ of sediment (min: 0, max: 38.8). Interpreting the classic peak component as occurrences
of fires, 50 fire episodes within the continuously sampled core segment, spanning the last c. 2200 yrs, were
identified. This results in a record-wide mean FRI of 43 yrs (min: 6, max: 594).

Classic and robust CHAR analysis distinguished four distinct phases, representing different states of the fire regime
(see Fig. 3). Phase 1 (c. 200 BCE to 600 CE) is characterised by relatively high CHAR of 0.83 ± 0.43 particles
300 cm^{-2} yr^{-1} and numerous (n = 23) peaks (i.e. fire episodes, Fig. 3c), with a SNI that is slightly above 3 for the most
part but slowly decreasing towards the following phase 2 (Fig. 3b). The mean FRI is 31 yrs (min: 6, max: 144).
Robust CHAR shows a steadily increasing background component (Fig. 3d), whereas both its peak component

15

(Fig. 3e) and sum (Fig. 3f) remain at low levels. More fire episodes (n = 16) occur in the following, shorter phase 2 (600–900 CE), with a lower mean FRI of c. 14 yrs. It incorporates some of the highest peaks of the whole record

305   with both the classic and robust approaches, resulting in a high CHAR of 1.3 ± 0.54 particles cm^{-2} yr^{-1} (including the maximum of 2.8 particles cm^{-2} yr^{-1}) while SNI falls below 3. In the transition to phase 3 at around 900 CE a pronounced decrease in charcoal input leads up to a long period of few to no fire episodes (n = 6) and longer mean FRI of >60 yrs (min: 6, max: 594). Hence, CHAR of phase 3 (900–1750 CE) is comparably low with 0.53 ± 0.29 particles cm^{-2} yr^{-1}, while robust CHAR background remains below average. The SNI decreases to a record-wide

310   minimum due to the lack of any CHAR peaks above the global threshold in the second half of phase 3. Finally, phase 4 (1750–2018 CE) has higher CHAR (0.61 ± 0.47 particles cm^{-2} yr^{-1}) and more frequent occurrences of fire episodes (n = 5), with mean FRI sharply decreasing to 40 yrs (min: 6, max: 78). An outstanding peak around 1880 CE leads to a maximum SNI >6 during this phase. Although phase 4 sees increasing CHAR and fire frequency after the low CHAR of phase 3, charcoal input decreases to a minimum within the last century (mean CHAR of

315   the last 100 yrs before core extraction = 0.56 ± 0.29 particles cm^{-2} yr^{-1}). In contrast, the robust CHAR background and sum show increases within phase 4 (Fig. 3d, e), and the robust peak component shows two maxima around the early 1800s and 1950 CE (Fig. 3e). In general, the older half of the record (c. 200 BCE to 1000 CE) has higher mean CHAR and a higher variability (0.97 ± 0.5 particles cm^{-2} yr^{-1}) compared to the younger half (1000–2018 CE; CHAR = 0.51 ± 0.32 particles cm^{-2} yr^{-1}). Even with added uncertainties from counting and the chronology, maxima

320   of robust CHAR mostly replicate periods of increased classic CHAR.

Over the entire record, 43.7% of charcoal particles belong to the smallest size class (150–300 µm), while 28.8% and 27.5% are part of the medium (300–500 µm) and large size classes (>500 µm), respectively. When assessed individually, more fire episodes are identified for smaller particles than for larger particles (Table 2).

The most prevalent morphotypes present in the sediment are types F (elongated, 31.7%), M (irregular, 28.4%), S

325   (angular, 20.6%), and B (angular, 7.2%), with all others (X, C, D, E, P) ranking at or below 3% each. Noticeably, two of the highest peaks of the record at c. 650 and 1880 CE are composed primarily of large (>500 µm), elongated (type F) particles. The total relative amount of type F particles seems to correlate with the largest particle size class, whereas type M is more closely associated with smaller particles (see Fig. 4 and Appendix B). Furthermore, the PCA indicates that there are rather weak grouping patterns of morphotype or size-class distributions in samples

330   of increasing core depth. The charcoal morphotypes show a similar temporal pattern for their background and peak components (Fig. 5c, d), mostly mirroring the decreased variability in the second half of the record as described for the sum of all particles.
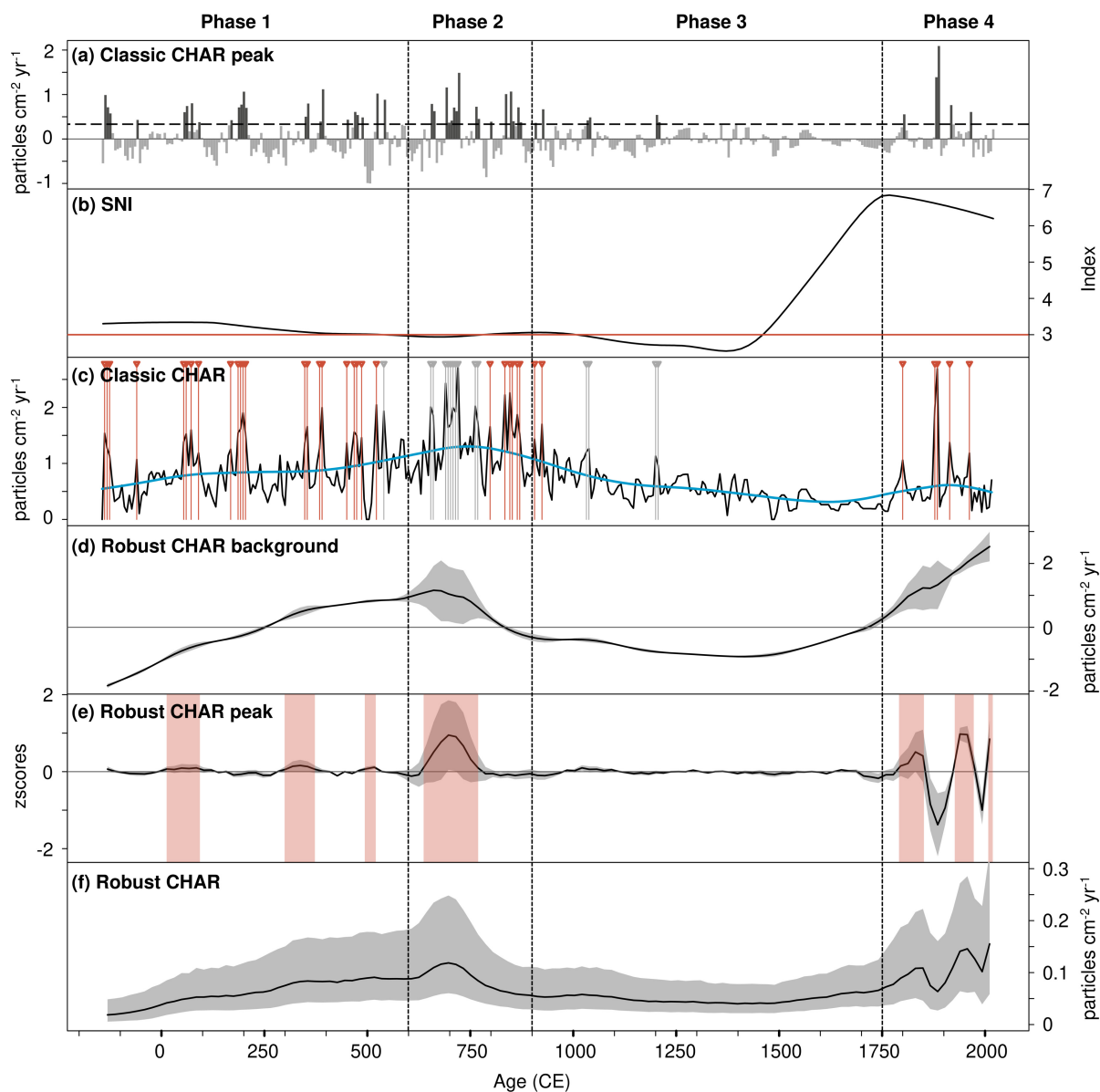
Figure 3: Overview of the charcoal record using classic and robust analysis approaches. Vertical dashed lines mark the
335 **different phases of the fire regime. (a) Classic CHAR peak component (dark grey bars = signal, light grey bars = noise,**
dashed horizontal line = threshold). (b) Signal-to-noise index (SNI) of the classic CHAR peak component after Kelly et
al. (2011) (red horizontal line = SNI cutoff value of 3). (c) Classic CHAR sum (black line = interpolated CHAR, blue line
= LOESS representing the CHAR background component, red vertical lines = fire episodes with SNI >3, grey vertical
lines = fire episodes with SNI <3). (d) Robust CHAR background component. (e) Robust CHAR peak component (red
340 **areas = above-average values). (f) Robust CHAR sum. For (d) – (f): black line = median, grey area = interquartile range.**

17

Particle class (share of total)	Samples with non-zero values	Identified fire episodes	FRI_{mean}	FRI_{max}	FRI_{min}	SNI >3 (%)
Elongated (36.2%)	261	25	80.3	726	6	82.8
Irregular (33.5%)	261	80	27.3	228	6	92.8
Angular (30.3%)	260	28	78.7	456	6	78.4
150–300 µm (43.7%)	287	57	37.5	372	6	65.1
300–500 µm (28.8%)	282	45	48.5	444	6	56.2
>500 µm (27.5%)	269	18	118.9	954	6	80.3
Total	300	50	42.9	594	6	68.1

Table 2: Reconstructed fire episodes, fire return interval (FRI) in years, and distributions of signal-to-noise index (SNI) >3 for charcoal morphotype and size classes, as well as the sum of charcoal particles over the last two millennia.
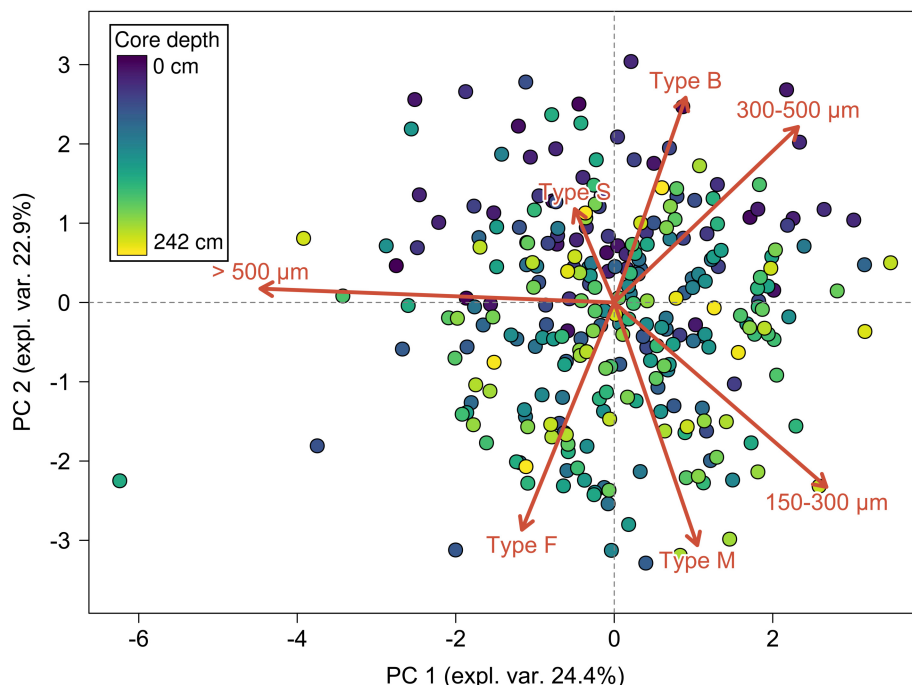
Figure 4: Principal component analysis (PCA) of charcoal particles (size classes and individual morphotypes with a share of >5% of the charcoal record).

3.3 Vegetation history

The pollen and NPP record, covering the whole sediment core and reaching back c. 2350 yrs, generally indicates a relatively stable vegetation composition (see Appendix A). The dominant arboreal pollen (AP) types comprise most of the pollen spectrum (average ratio of AP:NAP = 8.3:1) and reflect well the modern vegetation recorded around the lake, mostly *Pinus*, *Betula*, *Picea*, *Abies*, *Alnus,* and *Larix*, with smaller amounts of *Salix*, *Juniperus,* and *Populus*. Non-arboreal pollen (NAP) types are predominantly represented by Cyperaceae, followed by less abundant Poaceae, Ericales, and *Artemisia*. Despite similar general palynomorph distributions, maxima in the proportions of Cyperaceae and some evergreen tree pollen restricted to individual samples in the upper part of the record, lead to a separation into two pollen zones. Charcoal particles and pollen types have mostly weak correlations without statistical significance at *p* >0.05, although they hint at weak associations between irregular morphotypes with AP being contrasted by those of angular morphotypes and NAP (see Appendix B).

19

4 Discussion

4.1 Fire regime history of the last two millennia at Lake Khamra

The macroscopic charcoal record at Lake Khamra (Fig. 3) reveals gradually increasing, but relatively stable fire
360   activity from 200 BCE to 600 CE (phase 1). A period of high fire activity takes place between 600–900 CE,
expressed as higher CHAR and shorter FRIs (phase 2). It then transitions into an almost 600-year period without
any identified fire episodes and low CHAR (phase 3). From around 1750 CE the modern fire regime begins to take
shape (phase 4), with regularly identified fire episodes marking increasing fire frequency. However, the most
recent levels of CHAR are still lower than those of the maximum in phase 2 and reach a minimum in the 20th
365   century, meaning that the amount of modern charcoal accumulation is not unprecedented within the last c. 2200
yrs.

Robust CHAR (Fig. 3d–f), incorporating uncertainties from the age-depth model and charcoal counting,
necessarily loses the original charcoal record's short-term variability. It needs to be noted that any uncertainty
potentially arising from the assumed constant rate of old carbon input to the lake, underlying the sediment core's
370   chronology, is not included here, as any changes in magnitude of this reservoir-like effect are impossible to
quantify. This issue is common in studies in permafrost regions that use ^{14}C age dating (Biskaborn et al., 2012;
Colman et al., 1996; Nazarova et al., 2013; Vyse et al., 2020). In such instances, applying Pb/Cs age dating adds
valuable non-carbon-related estimates of sediment accumulation rates for the upper part of a sediment core
(Whitlock and Larsen, 2001).

375   The general trend of fire regime changes in SW Yakutia over the last c. 2200 yrs captured by the CHAR
background component (Fig. 5c) and described above, shares many similarities with a charcoal record from the
evergreen forest in the Tomsk region (c. 1500 km west of Lake Khamra; Feurdean et al., 2020). There, one period
of exceptionally high CHAR was observed around 700 CE and then again starting around 1700 CE towards the
present, in parallel with Lake Khamra's fire history. The onset of increased biomass burning around 1700 CE was
380   also reconstructed using aromatic acids from an ice core on the Severnaya Zemlya archipelago (c. 2200 km north-
west of Lake Khamra), and it indicates a sudden decrease at the beginning of the 20th century (Grieman et al.,
2017). However, the same study finds another maximum of biomass burning around 1500 CE, in contrast to a
clear period without fire episodes between c. 1250–1750 CE at Lake Khamra. Although comparisons across such
long distances and between different climate zones, archives, and fire proxies are likely to show differing results,
385   some of the described trends seem to be recorded at several sites worldwide. A global charcoal record synthesis
by Marlon et al. (2013) indicates decreasing biomass burning from c. 0 CE towards the industrial era, where, after

a maximum around 1850 CE, it decreases with the onset of the 20th century. Charcoal records from Siberia are underrepresented in such synthesis studies (Marlon et al., 2016), which, together with a lack of comparable records closer to SW Yakutia, underline the issue of sparse data in the region.

390 The reconstructed record-wide mean FRI of 43 yrs, incorporating both the exceptionally short FRI of phase 2 (14 yrs) and the long FRI of phase 3 (60 yrs, excluding the c. 600-yr-long period without identified fires), lies within the range of the few comparable studies in western Siberia. Barhoumi et al. (2019) found the shortest FRIs of the Holocene ranging from 40–100 yrs between 1500 CE and present day in macroscopic charcoal records from the northern Ural region. A mean FRI of 45 yrs during recent centuries was inferred by Feurdean et al. (2020). Other

395 studies using tree-stand ages and fire scars in tree-ring chronologies suggest mean FRIs of 80–90 yrs for mixed larch forests between the Yenisei and Tunguska rivers c. 1000 km north-west of Lake Khamra since c. 1800 CE, although the FRI of individual study sites could be as short as c. 50 yrs (Kharuk et al., 2008; Sofronov et al., 1998; Vaganov and Arbatskaya, 1996). A mean FRI of 52 yrs was reported for the northern Irkutsk region c. 300 km west of Lake Khamra in the 18th century (Wallenius et al., 2011) and 50–80 yrs for some sites in the north-eastern

400 larch-dominated forests (Kharuk et al., 2011; Schepaschenko et al., 2008). In general, FRIs increase with latitude due to lower incoming solar radiation, shorter fire seasons, and lower flammability of moist biomass (Kharuk, 2016; Kharuk et al., 2011), which likely contributes to a relatively short mean FRI at Lake Khamra. Additionally, studies of tree-ring chronologies or stand ages usually convey direct fire impact and are therefore more locally constrained, whereas a charcoal record incorporates fires from a larger source area (Remy et al., 2018).

405 Smaller charcoal particles record shorter FRIs than larger particles when analysing size classes individually (see Table 2 and Supplement), which could be because smaller particles have a larger source area, thus incorporating more fire events into the signal. However, the wide-spread assertion that larger charcoal particles generally originate from fires within a few hundred metres of the lake archive (Clark et al., 1998; Higuera et al., 2007; Ohlson and Tryterud, 2000) has been challenged (Peters and Higuera, 2007; Pisaric, 2002; Tinner et al., 2006;

410 Woodward and Haines, 2020). As wildfires in the Siberian boreal forest are predominantly considered low-intensity surface fires (de Groot et al., 2013), the potential of the resulting convection to transport large charcoal particles is probably limited compared to high-intensity crown fires. We therefore assume a charcoal source area of a few hundred metres around the lake for low-intensity fires (Conedera et al., 2009) and up to several kilometres for more intense fires producing stronger convection.

415 At Lake Khamra with a catchment to lake-area ratio of 23:1, the charcoal record predominantly consists of fragile morphotypes (types F, M, and S alone make up >80%). Enache and Cumming (2007) explain how a large catchment to lake-area ratio might favour secondary deposition of compact morphotypes, while fragile

morphotypes are more prone to fragmentation during surface runoff and thus rather represent primary input through the air. However, the present large catchment to lake-area ratio at Lake Khamra might indicate that

420   morphotype distribution is controlled by the type of biomass burning rather than secondary charcoal transport. This is also implied by the gentle and densely vegetated slopes that do not favour surface erosion.

Experimental charring studies have shown how different types of vegetation produce varied charcoal appearances (Jensen et al., 2007; Mustaphi and Pisaric, 2014; Pereboom et al., 2020). Pereboom et al. (2020) found elongated charcoal particles after experimentally burning tundra graminoids, but this result is likely not directly applicable

425   to a study site in the boreal forest. Noticeably, type F particles at Lake Khamra closely match the appearance of charred *Picea* needles reported by Mustaphi and Pisaric (2014). Together with the potential of more intense fires producing larger charcoal particles (Ward and Hardy, 1991), this could mean the two previously noted peaks of CHAR (c. 1880 CE at 19.5–20.5 cm depth and 650 CE at 124.5–125 cm; both dominated by high shares of type F particles >500 µm) are evidence of higher-intensity fires burning conifer trees more severely and within few

430   kilometres from the lake shore. Charring experiments with local vegetation and a regionally adapted morphotype classification scheme would potentially benefit future studies by providing clear ground-truthing for links between morphotypes and vegetation.

4.2 Drivers of fire regime variations

4.2.1 Vegetation

435   The overall stable vegetation composition during the time covered by the charcoal record, as implied by the pollen and NPP record (see Appendix A), indicates that vegetation changes were unlikely to be the main driver behind changes in the fire regime, and/or that changes in fire regime did not lead to large-scale shifts in vegetation composition. Similarly, no prominent shift in charcoal morphotype composition, and hence in the type of biomass burned over time, can be inferred (Fig. 5c, d). Although some studies draw a similar conclusion (e.g. Carcaillet et

440   al., 2001 in eastern Canada), this result contrasts with many other studies from the Eurasian and North American boreal zones, where vegetation changes were found to be closely connected to changes in fire regimes (Barhoumi et al., 2019, 2020; Feurdean et al., 2020; Gavin et al., 2007; Kelly et al., 2013). However, on a shorter, multi-decadal timescale, phases with more Cyperaceae pollen (sedges) in the Lake Khamra record and a higher ratio of evergreen to deciduous arboreal pollen types coincide with periods of high fire activity in phases 2 and 4 (see Fig.

445   5b). This could be due to either the ability of sedges to quickly settle on freshly disturbed and cleared out forest areas, and/or sedges growing in wetter areas, possibly right at the lake shore, which are spared by fires (Angelstam and Kuuluvainen, 2004; Isaev et al., 2010; Ivanova et al., 2014). Increased numbers of evergreen trees might enable

more intense crown fires. Indirectly, dry periods could lead to receding lake levels and thus an increase in both

shoreland sedges and fire ignitions. However, such clear links are difficult to infer without hydrological data. In

450   addition to differences in pollen source area and taphonomy compared to that of macroscopic charcoal, a variety

of factors likely obscures traces of potential fire impacts: surface fires in the deciduous forests in central Yakutia

mostly result in the elimination of only a share of a tree population depending on fire intensity (Matveev and

Usoltzev, 1996), while herbs or shrubs may recover too quickly for changes to be detected in our record with a

median temporal sampling resolution of 6 yrs and potential mixing processes and residence time of pollen grains

455   before settling in the lake sediment (Campbell, 1999; Fægri et al., 1989). These factors, together with a remaining

ambiguity in morphotype classification, likely explain the rather weak correlations of pollen and charcoal records.

4.2.2 Climate

The low fire activity in the latter half of phase 3 (900–1750 CE) overlaps with the Little Ice Age (LIA), when in

many regions of the Northern Hemisphere a cooler climate prevailed from c. 1400 to 1700 CE. In contrast, the

460   high fire activity during phase 2 pre-dates the proposed timing of the warmer Medieval Climate Anomaly (MCA)

lasting from c. 950 to 1250 CE by roughly 300 yrs (estimates of LIA and MCA durations from Mann et al., 2009).

Although it has been demonstrated that the timing and extent of these climatic phases are heterogeneous (Guiot et

al., 2010), evidence for their occurrence in Siberia is seen in other proxy studies (Churakova Sidorova et al., 2020;

Kharuk et al., 2010; Osborn and Briffa, 2006), albeit less pronounced when it comes to vegetation response in the

465   West Siberian Lowland (Philben et al., 2014). Neukom et al. (2019) show how these climatic periods arising from

averaged reconstructions at many individual study sites are not spatially or temporally coherent on the global scale,

and conclude that environmental reconstructions "should not be forced to fit into global narratives or epochs". This

might be especially true for studies using chronologies that have ^{14}C reservoir effects. Due to a lack of regional

studies, the PAGES Arctic 2k temperature reconstruction (McKay and Kaufman, 2014) was used to provide a

470   comparison between the reconstructed fire activity and large-scale changes in Arctic climate north of 60°N (Fig.

5a). This synthesis of circumpolar temperature reconstructions incorporates many records, although data from

Siberia are sparse and thus it is underrepresented compared to Greenland, North America, and Europe. However,

climate at Lake Khamra is likely to be strongly influenced by the conditions further north, as Arctic temperatures

affect the strength of the AO, which has been indirectly linked to fire activity further south (Balzter et al., 2005;

475   Kim et al., 2020). The reconstructed PAGES Arctic 2k temperature provides evidence for a colder climate around

c. 1600 CE, coinciding with the LIA and low fire activity at Lake Khamra. The following onset of increased fire

frequency in phase 4 is concurrent with a gradual increase in Arctic temperatures during the last two centuries

(Fig. 5a, c), although not exceeding the maximum in fire frequency of phase 2. The older half of the charcoal record (before c. 1000 CE) does not match the temperature reconstruction as clearly. This might be due to a more

480 regionally constrained climate, or a consequence of the lack of comparable data about humidity, which also affects fire activity (Brown and Giesecke, 2014; Power et al., 2008). A larch tree-ring based, c. 1500-yr-long reconstruction of summer vapour pressure deficit in north-eastern Yakutia (c. 2000 km from Lake Khamra) indicates that the modern, increasing level of drought stress is not yet unprecedented, being surpassed by a high vapour pressure deficit during the MCA (Churakova Sidorova et al., 2020). This is similar to trends observed in

485 the fire reconstruction at Lake Khamra. Another possibility for a less clear relationship between Arctic temperature and fire regime changes in the older half of the record is that the assumed constant impact of old carbon on the ^{14}C age dating might be less pronounced in this older millennium. Yet, an impact of colder Arctic temperatures on the reconstructed low fire activity in phase 2 at Lake Khamra seems likely and calls for more palaeoclimatic reconstructions and high-resolution charcoal records within the vicinity of the lake to better assess the role of

490 climate on shifts in the regional fire regime.

4.2.3 Human activity

The discrepancy of last century's low CHAR just after a phase of increasing fire frequency and rising Arctic temperature could potentially be a sign of direct and indirect consequences of human activity around Lake Khamra. The anthropogenic influence on fire regimes may be the most difficult to quantify due to missing information

495 about the kind and extent of human fire use and management throughout time, and the complex disentanglement of other drivers like climate and vegetation (Marlon et al., 2013). Although Lake Khamra is located in a sparsely populated region, humans have historically been shaping the surrounding landscapes by building forest winter tracks and roads (c. 0–30 km distance), logging (c. 10 km distance), and building villages and towns (ca. 30 and 40 km distance, respectively). Yakutia has been populated by humans since at least c. 28,000 BCE (Pitulko et al.,

500 2004), although the population first noticeably increased at the end of the LGM around 17,000 BCE (Fiedel and Kuzmin, 2007), eventually forming the indigenous hunting and reindeer herding tribes of Evens, Evenks, and Yukaghirs (Keyser et al., 2015; Pakendorf et al., 2006). Between 1100–1300 CE (in the first half of phase 3 in the charcoal record) the Sakha people moved in from the south, pressured by an expanding Mongol empire (Fedorova et al., 2013). They established a new and distinct form of semi-nomadic livelihood based on horse and cattle

505 breeding (Pakendorf et al., 1999). Fire was mainly used at hearths to provide warmth and light, but also to sustain grasslands for grazing (Kisilyakov, 2009; Pyne, 1996). Population density likely started to increase rapidly after Russian colonisation in the early 17th century (Crubézy et al., 2010), and even more drastically with the onset of

new industries like large-scale logging and mining in the 20th century (Pyne, 1996). When compared to the pastoralist societies that existed up to that point, anthropogenic influence on the fire regime likely increased at the

510   end of phase 3 (c. 1700 CE onwards) and throughout phase 4, after colonisation and industrialisation (Drobyshev et al., 2004). It has been shown that human livelihoods and the mentality towards fire use can often better explain shifts in fire regimes than population density alone (Bowman et al., 2011; Dietze et al., 2018). For example, a formerly smaller population could have relied on practices like slash-and-burn agriculture until there was a transition towards more industrialised, urban livelihoods and a new focus on active fire suppression to protect

515   forestry resources despite an increasing population (Dietze et al., 2019; Marlon et al., 2013). This is also thought to explain a pronounced decrease in boreal fire activity within the last century in tree ring studies from central Siberia (300 km west of Lake Khamra) and Fennoscandia (Wallenius, 2011; Wallenius et al., 2011). Forest roads and clearings could have acted as fire breaks, while the emergence of fire suppression in Russia was conceived as early as 1893 CE and later led to the founding of the first aerial firefighting unit in 1931 CE (Pyne, 1996). Adding

520   to this, slash-and-burn agriculture was officially banned at the end of the 18th century, but likely still practiced frequently up until the early 20th century (Drobyshev et al., 2004; Konakov, 1999; Kozubov and Taskaev, 1999). Higher fire frequency after c. 1750 CE, marking the onset of phase 4, therefore coincides with both a rapid increase in anthropogenic activity and land development, as well as a warming Arctic climate. Low CHAR within the last century on the other hand might be a consequence of a cultural shift towards seeing fire as a hazard to ban, control,

525   and suppress. Whereas high fire frequency in the past corresponded with high amounts of biomass burned, the recent century also sees increasing fire frequencies with decreasing total biomass burned (Fig. 5c, d). This might indicate that the current fire regime differs from that experienced by indigenous and Sakha people a few hundred years ago, now potentially consisting of more frequent, but smaller fires. A better understanding of fire use and management of the various Yakutian societies throughout history is needed to judge the extent of the human

530   influence on fire regimes in relatively remote regions, especially since it has the potential to obscure the effects of recent global warming in fire reconstructions.

Biogeosciences
Discussions
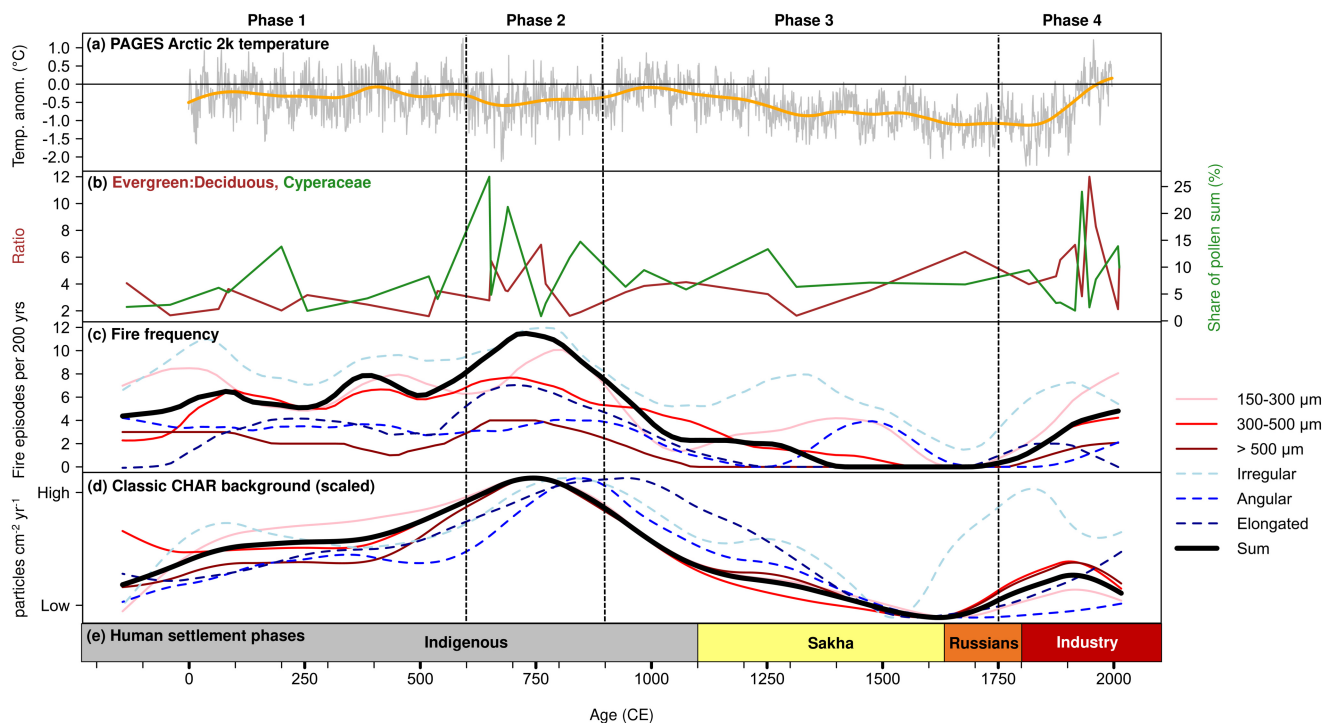
Figure 5: Comparison of the charcoal record with climate, vegetation, and general human settlement phases. Vertical dashed lines mark the different phases of the fire regime. (a) PAGES Arctic 2k temperature (grey line = original annual data, yellow line = LOESS). (b) Selected vegetation proxies. (c) Compiled, smoothed frequencies of fire episodes for the sum of particles and individual size classes/morphotypes. (d) Compiled classic CHAR background components for the sum of particles and individual size classes/morphotypes, scaled to equal extents for comparison. (e) General human settlement phases, referenced in the text. For (c)-(d): Lines represent size and morphotype classes as well as the sum of charcoal particles.

5 Conclusions

With its continuous sampling scheme and high median temporal resolution, the macroscopic charcoal record at Lake Khamra provides first insights into changes of the boreal fire regime of the last c. 2200 yrs in eastern Siberia, where comparable data are still lacking. Contrary to other studies, current levels of charcoal accumulation at Lake Khamra are not unprecedented within the last two millennia. The reconstructed fire regime changes do not coincide with large-scale shifts in vegetation composition, although short-term increases of evergreen trees and sedges broadly coincide with periods of increased biomass burning around 700 and 1850 CE (phases 2 and 4). Also, low fire activity from c. 900 to 1750 CE (phase 3), expressed as long FRIs and low charcoal accumulation, corresponds to a colder Arctic climate during the LIA. Despite the generally low population density, increased anthropogenic

Biogeosciences
Discussions
EGU
Open Access

forcing after the colonisation of Yakutia by the Russians in the early 17th century might have contributed to an
550   increase in fire frequency, together with rising temperatures. Although northern regions have been warming rapidly
in recent decades, charcoal input to the lake has been minimal during the last century, coinciding with new fire
management strategies and a ban on fire-related agricultural practices. The mean FRI of 43 yrs is at the lower end
of published literature for the wider region and incorporates a range of individual values of up to almost 600 yrs.
Overall charcoal accumulation (classic CHAR background component) and the frequency of identified fire
555   episodes seem to be directly related to each other for the majority of the record.

Although this new charcoal record improves data availability from eastern Siberia, more reconstructions,
especially from distinctly deciduous regions, are needed to form a detailed analysis of past fire regimes in the
Siberian boreal forest. An improved understanding of both fire activity and its drivers throughout history will
eventually enable a meaningful assessment of the presence and future of Siberian wildfires and their consequences.

560 **Appendix**
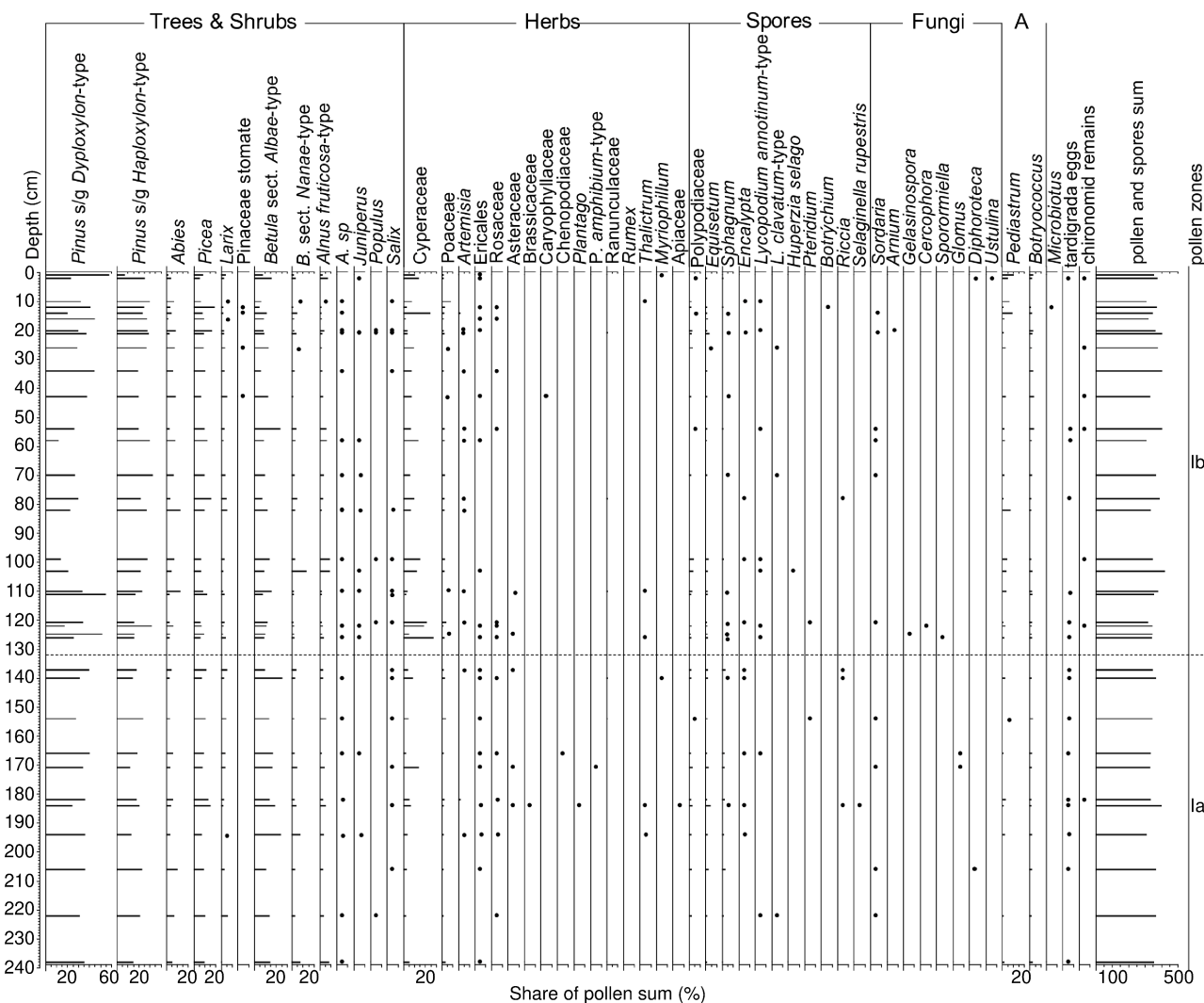
Appendix A: Pollen and non-pollen palynomorph record. Dots represent pollen taxa <1%.
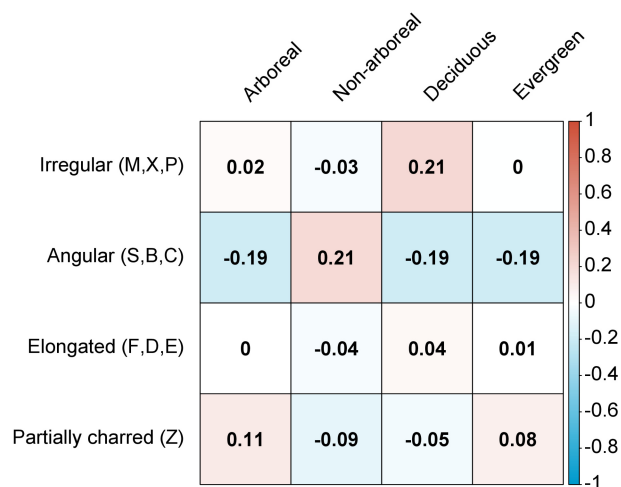
565   **Appendix B: Correlations (Kendall's τ) of charcoal morphotype classes with selected pollen groups.**

Code availability

The R script used to analyse the charcoal record presented in this study will be made permanently available on Zenodo and linked here. Review access to the script via GitHub: https://github.com/rglueckler/CharcoalAnalysisR

Data availability

570   The   data   presented   in   this   study   are   available   on   PANGAEA   at https://doi.pangaea.de/10.1594/PANGAEA.923773 (Glückler et al., 2020). Review access link: https://www.pangaea.de/tok/b54561820f2153ec0ce05c1e53efd086f8f5bfcd

Supplement

See separate Supplement file

575   **Author contribution**

ED and UH conceived and designed the study. LP, UH and SK organised the expedition to Yakutia. SV and BB collected the samples and conducted field measurements. RG and SV sampled the sediment core and performed the lab analysis. RG conducted all the charcoal proxy analysis, supported by ED and SK. AA conducted the pollen

and non-pollen palynomorph analysis. BW and ED analysed remote sensing data and created maps of the study
580 location. RG wrote the paper with inputs from ED. All the authors reviewed the final manuscript.

Competing interests

The authors declare that they have no conflict of interest.

References

590 Aakala, T., Pasanen, L., Helama, S., Vakkari, V., Drobyshev, I., Seppä, H., Kuuluvainen, T., Stivrins, N.,
Wallenius, T., Vasander, H. and Holmström, L.: Multiscale variation in drought controlled historical forest fire
activity in the boreal forests of eastern Fennoscandia, Ecol. Monogr., 88(1), 74–91,
https://doi.org/10.1002/ecm.1276, 2018.

Administrative Center Lensk: Lensky District Map, available at: https://mr-lenskij.sakha.gov.ru/o-rajone/karta-
595 lenskogo-rajona (last access: 21 October 2020), 2015

Alexander, H. D., Mack, M. C., Goetz, S., Beck, P. S. A. and Belshe, E. F.: Implications of increased deciduous
cover on stand structure and aboveground carbon pools of Alaskan boreal forests, Ecosphere, 3(5), 1–21,
https://doi.org/10.1890/ES11-00364.1, 2012.

Andreev, A. A., Morozova, E., Fedorov, G., Schirrmeister, L., Bobrov, A. A., Kienast, F. and Schwamborn, G.:
600 Vegetation history of central Chukotka deduced from permafrost paleoenvironmental records of the El'gygytgyn
Impact Crater, Clim. Past, 8(4), 1287–1300, https://doi.org/10.5194/cp-8-1287–2012, 2012.

Angelstam, P. and Kuuluvainen, T.: Boreal Forest Disturbance Regimes, Successional Dynamics and Landscape
Structures: A European Perspective, Ecological Bulletins, 51, 117–136, https://www.jstor.org/stable/20113303,
2004.

605 Appleby, P. G., Nolan, P. J., Gifford, D. W., Godfrey, M. J., Oldfield, F., Anderson, N. J. and Battarbee, R. W.:
^{210}Pb dating by low background gamma counting, Hydrobiologia, 143(1), 21–27, doi:10.1007/BF00026640, 1986.

Balzter, H., Gerard, F. F., George, C. T., Rowland, C. S., Jupp, T. E., McCallum, I., Shvidenko, A., Nilsson, S., Sukhinin, A., Onuchin, A. and Schmullius, C.: Impact of the Arctic Oscillation pattern on interannual forest fire variability in Central Siberia, Geophys. Res. Lett., 32(14), 1–4, https://doi.org/10.1029/2005GL022526, 2005.

610 Barhoumi, C., Peyron, O., Joannin, S., Subetto, D., Kryshen, A., Drobyshev, I., Girardin, M. P., Brossier, B., Paradis, L., Pastor, T., Alleaume, S. and Ali, A. A.: Gradually increasing forest fire activity during the Holocene in the northern Ural region (Komi Republic, Russia), The Holocene, 29(12), 1906–1920, https://doi.org/10.1177/0959683619865593, 2019.

Barhoumi, C., Ali, A. A., Peyron, O., Dugerdil, L., Borisova, O., Golubeva, Y., Subetto, D., Kryshen, A.,
615 Drobyshev, I., Ryzhkova, N. and Joannin, S.: Did long-term fire control the coniferous boreal forest composition of the northern Ural region (Komi Republic, Russia)?, J. Biogeogr., 1–16, https://doi.org/10.1111/jbi.13922, 2020.

Benaglia, T., Chauveau, D., Hunter, D. R. and Young, D.: mixtools: An R Package for analyzing finite mixture models. Journal of Statistical Software, 32(6), 1-29, available at http://www.jstatsoft.org/v32/i06/ (last access 21 October 2020), 2009

620
Biskaborn, B. K., Herzschuh, U., Bolshiyanov, D., Savelieva, L. and Diekmann, B.: Environmental variability in northeastern Siberia during the last ~13,300yr inferred from lake diatoms and sediment–geochemical parameters, Palaeogeogr. Palaeoclimatol. Palaeoecol., 329–330, 22–36, https://doi.org/10.1016/j.palaeo.2012.02.003, 2012.

Blarquez, O., Girardin, M. P., Leys, B., Ali, A. A., Aleman, J. C., Bergeron, Y. and Carcaillet, C.: Paleofire
625 reconstruction based on an ensemble-member strategy applied to sedimentary charcoal, Geophys. Res. Lett., 40(11), 2667–2672, https://doi.org/10.1002/grl.50504, 2013.

Blaauw, M., Christen, A. and Aquino L., M. A.: rbacon: Age-Depth Modelling using Bayesian Statistics. R package version 2.4.3, available at https://CRAN.R-project.org/package=rbacon (last access: 21 October 2020), 2020

630
Blaauw, M. and Christen, J. A.: 2011 Flexible paleoclimate age-depth models using an autoregressive gamma process, Bayesian Anal., 6(3), 457–474, https://doi.org/10.1214/11-BA618, 2011

Blarquez, O., Vannière, B., Marlon, J. R., Daniau, A.-L., Power, M. J., Brewer, S. and Bartlein, P. J.: paleofire:
635 An R package to analyse sedimentary charcoal records from the Global Charcoal Database to reconstruct past biomass burning, Comput. Geosci., 72, 255–261, https://doi.org/10.1016/j.cageo.2014.07.020, 2014.

Bouchard, F., MacDonald, L. A., Turner, K. W., Thienpont, J. R., Medeiros, A. S., Biskaborn, B. K., Korosi, J., Hall, R. I., Pienitz, R. and Wolfe, B. B.: Paleolimnology of thermokarst lakes: a window into permafrost landscape evolution, Arct. Sci., 3, 91–117, https://doi.org/10.1139/as-2016-0022, 2016.

640 Bowman, D. M. J. S., Balch, J., Artaxo, P., Bond, W. J., Cochrane, M. A., D'Antonio, C. M., DeFries, R., Johnston, F. H., Keeley, J. E., Krawchuk, M. A., Kull, C. A., Mack, M., Moritz, M. A., Pyne, S., Roos, C. I., Scott, A. C., Sodhi, N. S. and Swetnam, T. W.: The human dimension of fire regimes on Earth, J. Biogeogr., 38(12), 2223–2236, https://doi.org/10.1111/j.1365-2699.2011.02595.x, 2011.

Brown, K. J. and Giesecke, T.: Holocene fire disturbance in the boreal forest of central Sweden, Boreas, 43(3),
645   639–651, https://doi.org/10.1111/bor.12056, 2014.

Brunelle, A. and Anderson, R. S.: Sedimentary charcoal as an indicator of late-Holocene drought in the Sierra
Nevada,   California,   and   its   relevance   to   the   future,   The   Holocene,   13(1),   21–28,
https://doi.org/10.1191/0959683603hl591rp, 2003.

Campbell, I. D.: Quaternary pollen taphonomy: examples of differential redeposition and differential preservation,
650   Palaeogeogr. Palaeoclimatol. Palaeoecol., 149(1), 245–256, https://doi.org/10.1016/S0031-0182(98)00204-1,
1999.

Carcaillet, C., Bergeron, Y., Richard, P. J. H., Fréchette, B., Gauthier, S. and Prairie, Y. T.: Change of fire
frequency in the eastern Canadian boreal forests during the Holocene: does vegetation composition or climate
trigger the fire regime?, J. Ecol., 89(6), 930–946, https://doi.org/10.1111/j.1365-2745.2001.00614.x, 2001.

655   Chelnokova, S. M., Chikina, I. D. and Radchenko, S. A.: Geologic map of Yakutia P-48,49, 1:1.000.000, VSEGEI,
Leningrad,   available   at   http://www.geokniga.org/sites/geokniga/files/maps/p-4849-vanavara-gosudarstvennaya-
geologicheskaya-karta-sssr-novaya-seriya-karta-_0.jpg (last access: 21 October 2020),1988

Churakova Sidorova, O. V., Corona, C., Fonti, M. V., Guillet, S., Saurer, M., Siegwolf, R. T. W., Stoffel, M. and
660   Vaganov, E. A.: Recent atmospheric drying in Siberia is not unprecedented over the last 1,500 years, Sci. Rep.,
10(1), https://doi.org/10.1038/s41598-020-71656-w, 2020.

Clark, J. S.: Particle motion and the theory of charcoal analysis: Source area, transport, deposition, and sampling,
Quat. Res., 30(1), 67–80, doi:10.1016/0033-5894(88)90088-9, 1988.

Clark, J. S., Lynch, J., Stocks, B. J. and Goldammer, J. G.: Relationships between charcoal particles in air and
665   sediments in west-central Siberia, The Holocene, 8(1), 19–29, https://doi.org/10.1191/095968398672501165,
1998.

Colman, S. M., Jones, G. A., Rubin, M., King, J. W., Peck, J. A. and Orem, W. H.: AMS radiocarbon analyses
from Lake Baikal, Siberia: Challenges of dating sediments from a large oligotrophic lake, Quat. Sci. Rev., 15(7),
669–684, https://doi.org/10.1016/0277-3791(96)00027-3, 1996.

670   Conedera, M., Tinner, W., Neff, C., Meurer, M., Dickens, A. F. and Krebs, P.: Reconstructing past fire regimes:
methods, applications, and relevance to fire management and conservation, Quat. Sci. Rev., 28(5), 555–576,
https://doi.org/10.1016/j.quascirev.2008.11.005, 2009.

Crubézy, E., Amory, S., Keyser, C., Bouakaze, C., Bodner, M., Gibert, M., Röck, A., Parson, W., Alexeev, A. and
Ludes, B.: Human evolution in Siberia: from frozen bodies to ancient DNA, BMC Evol. Biol., 10(25), 1–16,
675   https://doi.org/10.1186/1471-2148-10-25, 2010.

Dietze, E., Theuerkauf, M., Bloom, K., Brauer, A., Dörfler, W., Feeser, I., Feurdean, A., Gedminienė, L., Giesecke,
T., Jahns, S., Karpińska-Kołaczek, M., Kołaczek, P., Lamentowicz, M., Latałowa, M., Marcisz, K., Obremska,
M., Pędziszewska, A., Poska, A., Rehfeld, K., Stančikaitė, M., Stivrins, N., Święta-Musznicka, J., Szal, M.,
Vassiljev, J., Veski, S., Wacnik, A., Weisbrodt, D., Wiethold, J., Vannière, B. and Słowiński, M.: Holocene fire

680   activity during low-natural flammability periods reveals scale-dependent cultural human-fire relationships in Europe, Quat. Sci. Rev., 201, 44–56, https://doi.org/10.1016/j.quascirev.2018.10.005, 2018.

Dietze, E., Brykała, D., Schreuder, L. T., Jażdżewski, K., Blarquez, O., Brauer, A., Dietze, M., Obremska, M., Ott, F., Pieńczewska, A., Schouten, S., Hopmans, E. C. and Słowiński, M.: Human-induced fire regime shifts during 19th century industrialization: A robust fire regime reconstruction using northern Polish lake sediments, PLOS
685   ONE, 14(9), 1–20, https://doi.org/10.1371/journal.pone.0222011, 2019.

Dietze, E., Mangelsdorf, K., Andreev, A., Karger, C., Schreuder, L. T., Hopmans, E. C., Rach, O., Sachse, D., Wennrich, V. and Herzschuh, U.: Relationships between low-temperature fires, climate and vegetation during three late glacials and interglacials of the last 430 kyr in northeastern Siberia reconstructed from monosaccharide anhydrides in Lake El'gygytgyn sediments, Clim. Past, 16, 799–818, https://doi.org/10.5194/cp-16-799-2020,
690   2020.

Drobyshev, I., Niklasson, M., Angelstam, P. and Majewski, P.: Testing for anthropogenic influence on fire regime for a 600-year period in the Jaksha area, Komi Republic, East European Russia, Can. J. For. Res., 34, 2027–2036, https://doi.org/10.1139/X04-081, 2004.

Duffin, K. I., Gillson, L. and Willis, K. J.: Testing the sensitivity of charcoal as an indicator of fire events in
695   savanna environments: quantitative predictions of fire proximity, area and intensity, The Holocene, 18(2), 279–291, https://doi.org/10.1177/0959683607086766, 2008.

Ehlers, J. and Gibbard, P. L.: The extent and chronology of Cenozoic Global Glaciation, Quat. Int., 164–165, 6–20, https://doi.org/10.1016/j.quaint.2006.10.008, 2007.

Enache, M. D. and Cumming, B. F.: Charcoal morphotypes in lake sediments from British Columbia (Canada): an
700   assessment of their utility for the reconstruction of past fire and precipitation, J. Paleolimnol., 38(3), 347–363, https://doi.org/10.1007/s10933-006-9084-8, 2007.

Fægri, K., Iversen, J., Kaland, P. E. and Krzywinski, K.: Textbook of pollen analysis. (Ed. 4), John Wiley & Sons Ltd., Chichester, UK, 1989.

Fedorov, A. N., Vasilyev, N. F., Torgovkin, Y. I., Shestakova, A. A., Varlamov, S. P., Zheleznyak, M. N.,
705   Shepelev, V. V., Konstantinov, P. Y., Kalinicheva, S. S., Basharin, N. I., Makarov, V. S., Ugarov, I. S., Efremov, P. V., Argunov, R. N., Egorova, L. S., Samsonova, V. V., Shepelev, A. G., Vasiliev, A. I., Ivanova, R. N., Galanin, A. A., Lytkin, V. M., Kuzmin, G. P. and Kunitsky, V. V.: Permafrost-Landscape Map of the Republic of Sakha (Yakutia) on a Scale 1:1,500,000, Geosciences, 8(12), 1–17, https://doi.org/10.3390/geosciences8120465, 2018.

Fedorova, S. A., Reidla, M., Metspalu, E., Metspalu, M., Rootsi, S., Tambets, K., Trofimova, N., Zhadanov, S. I.,
710   Kashani, B. H., Olivieri, A., Voevoda, M. I., Osipova, L. P., Platonov, F. A., Tomsky, M. I., Khusnutdinova, E. K., Torroni, A. and Villems, R.: Autosomal and uniparental portraits of the native populations of Sakha (Yakutia): implications for the peopling of Northeast Eurasia, BMC Evol. Biol., 13, 1–18, https://doi.org/10.1186/1471-2148-13-127, 2013.

Feurdean, A., Veski, S., Florescu, G., Vannière, B., Pfeiffer, M., O'Hara, R. B., Stivrins, N., Amon, L., Heinsalu,
715   A., Vassiljev, J. and Hickler, T.: Broadleaf deciduous forest counterbalanced the direct effect of climate on

Holocene fire regime in hemiboreal/boreal region (NE Europe), Quat. Sci. Rev., 169, 378–390, https://doi.org/10.1016/j.quascirev.2017.05.024, 2017.

Feurdean, A., Florescu, G., Tanţău, I., Vannière, B., Diaconu, A.-C., Pfeiffer, M., Warren, D., Hutchinson, S. M., Gorina, N., Gałka, M. and Kirpotin, S.: Recent fire regime in the southern boreal forests of western Siberia is
720 unprecedented   in   the   last   five   millennia,   Quat.   Sci.   Rev.,   244,   1–16, https://doi.org/10.1016/j.quascirev.2020.106495, 2020.

Fiedel, S. J. and Kuzmin, Y. V.: Radiocarbon date frequency as an index of intensity of paleolithic occupation of Siberia: did humans react predictably to climate oscillations?, Radiocarbon, 49(2), 741–756, https://doi.org/https://doi.org/10.1017/S0033822200042624, 2007.

725 Flannigan, M., Stocks, B., Turetsky, M. and Wotton, M.: Impacts of climate change on fire activity and fire management in the circumboreal forest, Glob. Change Biol., 15(3), 549–560, https://doi.org/10.1111/j.1365-2486.2008.01660.x, 2009.

Frégeau, M., Payette, S. and Grondin, P.: Fire history of the central boreal forest in eastern North America reveals stability since the mid-Holocene, The Holocene, 25(12), 1912–1922, https://doi.org/10.1177/0959683615591361,
730 2015.

Gavin, D. G., Hallett, D. J., Hu, F. S., Lertzman, K. P., Prichard, S. J., Brown, K. J., Lynch, J. A., Bartlein, P. and Peterson, D. L.: Forest fire and climate change in western North America: insights from sediment charcoal records, Front. Ecol. Environ., 5(9), 499–506, https://doi.org/10.1890/060161, 2007.

Goldammer, J. G. and Furyaev, V. V.: Fire in Ecosystems of Boreal Eurasia: Ecological Impacts and Links to the
735 Global System, in Fire in Ecosystems of Boreal Eurasia, edited by J. G. Goldammer and V. V. Furyaev, pp. 1–20, Springer Netherlands, Dordrecht, 1996.

Grieman, M. M., Aydin, M., Fritzsche, D., McConnell, J. R., Opel, T., Sigl, M. and Saltzman, E. S.: Aromatic acids in a Eurasian Arctic ice core: a 2600-year proxy record of biomass burning, Clim Past, 16, 395–410, https://doi.org/10.5194/cp-13-395-2017, 2017.

740 de Groot, W. J., Cantin, A. S., Flannigan, M. D., Soja, A. J., Gowman, L. M. and Newbery, A.: A comparison of Canadian   and   Russian   boreal   forest   fire   regimes,   For.   Ecol.   Manag.,   294,   23–34, https://doi.org/10.1016/j.foreco.2012.07.033, 2013.

Glückler, R., Herzschuh, U., Vyse, S. A., Dietze, E.: Macroscopic charcoal record from Lake Khamra, Yakutia, Russia, available at: https://doi.pangaea.de/10.1594/PANGAEA.923773, 2020
745

Grosse, G., Jones, B. and Arp, C.: 8.21 Thermokarst Lakes, Drainage, and Drained Basins, in Treatise on Geomorphology, edited by J. F. Shroder, pp. 325–353, Academic Press, San Diego, 2013.

Guiot, J., Corona, C. and ESCARSEL members: Growing season temperatures in Europe and Climate forcings over the past 1400 years, PLOS ONE, 5(4), 1–15, https://doi.org/10.1371/journal.pone.0009972, 2010.

750   Hajdas, I., Zolitschka, B., Bonani, G., Leroy, S. A. G., Negendank, J. W., Ramratht, M. and Suter, M.: AMS radiocarbon dating of annually laminated sediments from lake Holzmaar, Germany, Quat. Sci. Rev., 14, 137–143, 1995.

Halsall, K. M., Ellingsen, V. M., Asplund, J., Bradshaw, R. H. and Ohlson, M.: Fossil charcoal quantification using manual and image analysis approaches, The Holocene, 28(8), 1345–1353,
755   https://doi.org/10.1177/0959683618771488, 2018.

Hansen, M. C., Potapov, P. V., Moore, R., Hancher, M., Turubanova, S. A., Tyukavina, A., Thau, D., Stehman, S. V., Goetz, S. J., Loveland, T. R., Kommareddy, A., Egorov, A., Chini, L., Justice, C. O. and Townshend, J. R. G.: High-resolution global maps of 21st-century forest cover change, Science, 342, 850–853, https://doi.org/10.1126/science.1244693, 2013.

760   Hawthorne, D., Courtney Mustaphi, C. J., Aleman, J. C., Blarquez, O., Colombaroli, D., Daniau, A.-L., Marlon, J. R., Power, M., Vannière, B., Han, Y., Hantson, S., Kehrwald, N., Magi, B., Yue, X., Carcaillet, C., Marchant, R., Ogunkoya, A., Githumbi, E. N. and Muriuki, R. M.: Global Modern Charcoal Dataset (GMCD): A tool for exploring proxy-fire linkages and spatial patterns of biomass burning, Quat. Int., 488, 3–17, https://doi.org/10.1016/j.quaint.2017.03.046, 2018.

765   Hély, C., Girardin, M. P., Ali, A. A., Carcaillet, C., Brewer, S. and Bergeron, Y.: Eastern boreal North American wildfire risk of the past 7000 years: A model-data comparison, Geophys. Res. Lett., 37(14), 1–6, https://doi.org/10.1029/2010GL043706, 2010.

Herzschuh, U.: Legacy of the Last Glacial on the present-day distribution of deciduous versus evergreen boreal forests, Glob. Ecol. Biogeogr., 29(2), 198–206, https://doi.org/10.1111/geb.13018, 2020.

770   Herzschuh, U., Birks, H. J. B., Laepple, T., Andreev, A., Melles, M. and Brigham-Grette, J.: Glacial legacies on interglacial vegetation at the Pliocene-Pleistocene transition in NE Asia, Nat. Commun., 7(1), 1–11, https://doi.org/10.1038/ncomms11967, 2016.

Higuera, P. E., Peters, M. E., Brubaker, L. B. and Gavin, D. G.: Understanding the origin and analysis of sediment-charcoal records with a simulation model, Quat. Sci. Rev., 26(13), 1790–1809,
775   https://doi.org/10.1016/j.quascirev.2007.03.010, 2007.

Higuera, P. E., Brubaker, L. B., Anderson, P. M., Hu, F. S. and Brown, T. A.: Vegetation mediated the impacts of postglacial climate change on fire regimes in the south-central Brooks Range, Alaska, Ecol. Monogr., 79(2), 201–219, https://doi.org/10.1890/07-2019.1, 2009.

Hoecker, T. J., Higuera, P. E., Kelly, R. and Hu, F. S.: Arctic and boreal paleofire records reveal drivers of fire
780   activity and departures from Holocene variability, Ecology, 101(9), 1–17, https://doi.org/10.1002/ecy.3096, 2020.

Hudspith, V. A., Belcher, C. M., Kelly, R. and Hu, F. S.: Charcoal reflectance reveals early Holocene boreal deciduous forests burned at high intensities, PLOS ONE, 10(4), e0120835, https://doi.org/10.1371/journal.pone.0120835, 2015.

785 Isaev, A. P., Protopopov, A. V., Protopopova, V. V., Egorova, A. A., Timofeyev, P. A., Nikolaev, A. N., Shurduk, I. F., Lytkina, L. P., Ermakov, N. B., Nikitina, N. V., Efimova, A. P., Zakharova, V. I., Cherosov, M. M., Nikolin, E. G., Sosina, N. K., Troeva, E. I., Gogoleva, P. A., Kuznetsova, L. V., Pestryakov, B. N., Mironova, S. I. and Sleptsova, N. P.: Vegetation of Yakutia: Elements of Ecology and Plant Sociology, in The Far North: Plant Biodiversity and Ecology of Yakutia, edited by E. I. Troeva, A. P. Isaev, M. M. Cherosov and N.S. Karpov, pp. 143–260, https://doi.org/10.1007/978-90-481-3774-9_3, Springer Science+Business Media B.V., 2010

790 Ito, A.: Modelling of carbon cycle and fire regime in an east Siberian larch forest, Ecol. Model., 187(2), 121–139, https://doi.org/10.1016/j.ecolmodel.2005.01.037, 2005.

Ivanova, A. A., Kopylova-Guskova, E. O., Shipunov, A. B. and Volkova, P. A.: Post-fire succession in the northern pine forest in Russia: a case study, Wulfenia, 21, 119–128, 2014.

Jansen, E., Christensen, J. H., Dokken, T., Nisancioglu, K. H., Vinther, B. M., Capron, E., Guo, C., Jensen, M. F., 795 Langen, P. L., Pedersen, R. A., Yang, S., Bentsen, M., Kjær, H. A., Sadatzki, H., Sessford, E. and Stendel, M.: Past perspectives on the present era of abrupt Arctic climate change, Nat. Clim. Change, 10(8), 714–721, https://doi.org/10.1038/s41558-020-0860-7, 2020.

Jensen, K., Lynch, E. A., Calcote, R. and Hotchkiss, S. C.: Interpretation of charcoal morphotypes in sediments from Ferry Lake, Wisconsin, USA: do different plant fuel sources produce distinctive charcoal morphotypes?, The 800 Holocene, 17(7), 907–915, https://doi.org/10.1177/0959683607082405, 2007.

Katamura, F., Fukuda, M., Bosikov, N. P. and Desyatkin, R. V.: Charcoal records from thermokarst deposits in central Yakutia, eastern Siberia: Implications for forest fire history and thermokarst development, Quat. Res., 71(1), 36–40, https://doi.org/10.1016/j.yqres.2008.08.003, 2009a.

Katamura, F., Fukuda, M., Bosikov, N. P. and Desyatkin, R. V.: Forest fires and vegetation during the Holocene 805 in central Yakutia, eastern Siberia, J. For. Res., 14(1), 30–36, https://doi.org/10.1007/s10310-008-0099-z, 2009b.

Keaveney, E. M. and Reimer, P. J.: Understanding the variability in freshwater radiocarbon reservoir offsets: a cautionary tale, J. Archaeol. Sci., 39(5), 1306–1316, https://doi.org/10.1016/j.jas.2011.12.025, 2012.

Kelly, R., Chipman, M. L., Higuera, P. E., Stefanova, I., Brubaker, L. B. and Hu, F. S.: Recent burning of boreal forests exceeds fire regime limits of the past 10,000 years, Proc. Natl. Acad. Sci., 110(32), 13055–13060, 810 https://doi.org/10.1073/pnas.1305069110, 2013.

Kelly, R. F., Higuera, P. E., Barrett, C. M. and Hu, F. S.: A signal-to-noise index to quantify the potential for peak detection in sediment–charcoal records, Quat. Res., 75(1), 11–17, https://doi.org/10.1016/j.yqres.2010.07.011, 2011.

Keyser, C., Hollard, C., Gonzalez, A., Fausser, J.-L., Rivals, E., Alexeev, A. N., Riberon, A., Crubézy, E. and 815 Ludes, B.: The ancient Yakuts: a population genetic enigma, Philos. Trans. R. Soc., 370, 20130385, https://doi.org/10.1098/rstb.2013.0385, 2015.

Kharuk, V. I.: Larch forests of Middle Siberia: long-term trends in fire return intervals, Reg Environ Change, 16, 2389–2397, https://doi.org/10.1007/s10113-016-0964-9, 2016.

Kharuk, V. I., Ranson, K. J. and Dvinskaya, M. L.: Wildfires dynamic in the larch dominance zone, Geophys. Res.
820   Lett., 35(1), L01402, https://doi.org/10.1029/2007GL032291, 2008.

Kharuk, V. I., Im, S. T., Dvinskaya, M. L. and Ranson, K. J.: Climate-induced mountain tree-line evolution in
southern Siberia, Scand. J. For. Res., 25(5), 446–454, https://doi.org/10.1080/02827581.2010.509329, 2010.

Kharuk, V. I., Ranson, K. J., Dvinskaya, M. L. and Im, S. T.: Wildfires in northern Siberian larch dominated
communities, Environ. Res. Lett., 6(4), 045208, https://doi.org/10.1088/1748-9326/6/4/045208, 2011.

825   Kim, J.-S., Kug, J.-S., Jeong, S.-J., Park, H. and Schaepman-Strub, G.: Extensive fires in southeastern Siberian
permafrost   linked   to   preceding   Arctic   Oscillation,   Sci.   Adv.,   6(2),   eaax3308,
https://doi.org/10.1126/sciadv.aax3308, 2020.

Kisilyakov, Y.: Prescribed Fire Experiments in Krasnoyarsk Region, Russia, IFFN, 38, 51–62, 2009

Konakov, N. D.: Agriculture. In Traditional culture of European North-East of Russia, available at
830   http://www.komi.com/Folk/komi/txt84.htm (last access 21 October 2020), 1999.

Köster, E., Köster, K., Berninger, F., Prokushkin, A., Aaltonen, H., Zhou, X. and Pumpanen, J.: Changes in fluxes
of carbon dioxide and methane caused by fire in Siberian boreal forest with continuous permafrost, J. Environ.
Manage., 228, 405–415, https://doi.org/10.1016/j.jenvman.2018.09.051, 2018.

835   Kozubov, G. M. and Taskaev, A. I.: Forestry and forest resources of Komi republic, DiK Publishing House,

Moscow, 1999

Kruse, S., Bolshiyanov, D., Grigoriev, M. N., Morgenstern, A., Pestryakova, L., Tsibizov, L. and Udke, A.:
Russian-German   Cooperation: Expeditions   to   Siberia   in   2018,   Rep.   Polar   Mar.   Res.,
https://doi.org/10.2312/BzPM_0734_2019, 2019.

840   Kuuluvainen, T. and Gauthier, S.: Young and old forest in the boreal: critical stages of ecosystem dynamics and
management under global change, For. Ecosyst., 5(1), 1–15, https://doi.org/10.1186/s40663-018-0142-2, 2018.

Lenton, T. M.: Arctic climate tipping points, Ambio, 41(1), 10–22, https://doi.org/10.1007/s13280-011-0221-x,
2012.

Lenton, T. M., Held, H., Kriegler, E., Hall, J. W., Lucht, W., Rahmstorf, S. and Schellnhuber, H. J.: Tipping
845   elements in the Earth's climate system, PNAS, 105(6), 1786–1793, https://doi.org/10.1073/pnas.0705414105,
2008.

Leys, B., Brewer, S. C., McConaghy, S., Mueller, J. and McLauchlan, K. K.: Fire history reconstruction in
grassland ecosystems: amount of charcoal reflects local area burned, Environ. Res. Lett., 10(11), 114009,
https://doi.org/10.1088/1748-9326/10/11/114009, 2015.

850   Loader, C.: locfit: Local Regression, Likelihood and Density Estimation. R package version 1.5-9.4, available at
https://CRAN.R-project.org/package=locfit (last access 21 October 2020), 2020

Mann, M. E., Zhang, Z., Rutherford, S., Bradley, R. S., Hughes, M. K., Shindell, D., Ammann, C., Faluvegi, G. and Ni, F.: Global signatures and dynamical origins of the Little Ice Age and Medieval Climate Anomaly, Science, 855 326(5957), 1256–1260, https://doi.org/10.1126/science.1177303, 2009.

Marlon, J. R., Bartlein, P. J., Carcaillet, C., Gavin, D. G., Harrison, S. P., Higuera, P. E., Joos, F., Power, M. J. and Prentice, I. C.: Climate and human influences on global biomass burning over the past two millennia, Nat. Geosci., 1(10), 697–702, https://doi.org/10.1038/ngeo313, 2008.

Marlon, J. R., Bartlein, P. J., Daniau, A.-L., Harrison, S. P., Maezumi, S. Y., Power, M. J., Tinner, W. and 860 Vanniére, B.: Global biomass burning: a synthesis and review of Holocene paleofire records and their controls, Quat. Sci. Rev., 65, 5–25, https://doi.org/10.1016/j.quascirev.2012.11.029, 2013.

Marlon, J. R., Kelly, R., Daniau, A.-L., Vannière, B., Power, M. J., Bartlein, P., Higuera, P., Blarquez, O., Brewer, S., Brücher, T., Feurdean, A., Romera, G. G., Iglesias, V., Maezumi, S. Y., Magi, B., Mustaphi, C. J. C. and Zhihai, T.: Reconstructions of biomass burning from sediment-charcoal records to improve data–model comparisons, 865 Biogeosciences, 13, 3225–3244, https://doi.org/10.5194/bg-13-3225-2016, 2016.

Matveev, P. M. and Usoltzev, V. A.: Post-fire mortality and regeneration of *Larix sibirica* and *Larix dahurica* in conditions of long-term permafrost, in Fire in Ecosystems of Boreal Eurasia, edited by J. G. Goldammer and V. V. Furyaev, pp. 366–371, Springer Netherlands, Dordrecht, 1996.

McKay, N. P. and Kaufman, D. S.: An extended Arctic proxy temperature database for the past 2,000 years, Sci. 870 Data, 140026, https://doi.org/10.1038/sdata.2014.26, 2014.

Molinari, C., Carcaillet, C., Bradshaw, R. H. W., Hannon, G. E. and Lehsten, V.: Fire-vegetation interactions during the last 11,000 years in boreal and cold temperate forests of Fennoscandia, Quat. Sci. Rev., 241, 106408, https://doi.org/10.1016/j.quascirev.2020.106408, 2020.

Mustaphi, C. J. C. and Pisaric, M. F. J.: A classification for macroscopic charcoal morphologies found in Holocene 875 lacustrine sediments, Prog. Phys. Geogr. Earth Environ., 38(6), 734–754, https://doi.org/10.1177/0309133314548886, 2014.

Nazarova, L., Lüpfert, H., Subetto, D., Pestryakova, L. and Diekmann, B.: Holocene climate conditions in central Yakutia (Eastern Siberia) inferred from sediment composition and fossil chironomids of Lake Temje, Quat. Int., 290–291, 264–274, https://doi.org/10.1016/j.quaint.2012.11.006, 2013.

880 Neukom, R., Steiger, N., Gómez-Navarro, J. J., Wang, J. and Werner, J. P.: No evidence for globally coherent warm and cold periods over the preindustrial Common Era, Nature, 571(7766), 550–554, https://doi.org/10.1038/s41586-019-1401-2, 2019.

Nilsson, S. and Shvidenko, A.: Is sustainable development of the Russian forest sector possible?, IUFRO, 11, Vienna, Austria, 1996

885

Ohlson, M. and Tryterud, E.: Interpretation of the charcoal record in forest soils: forest fires and their production and deposition of macroscopic charcoal, The Holocene, 10(4), 519–525, https://doi.org/10.1191/095968300667442551, 2000.

890 Osborn, T. J. and Briffa, K. R.: The spatial extent of 20th-century warmth in the context of the past 1200 years, Science, 311(5762), 841–844, https://doi.org/10.1126/science.1120514, 2006.

Pakendorf, B., Spitsyn, V. A. and Rodewald, A.: Genetic structure of a Sakha population from Siberia and ethnic affinities, Hum. Biol., 71(2), 231–244, 1999.

Pakendorf, B., Novgorodov, I. N., Osakovskij, V. L., Danilova, A. P., Protodjakonov, A. P. and Stoneking, M.: Investigating the effects of prehistoric migrations in Siberia: genetic variation and the origins of Yakuts, Hum
895 Genet, 20, 334–353, https://doi.org/10.1007/s00439-006-0213-2, 2006.

Pereboom, E. M., Vachula, R. S., Huang, Y. and Russell, J.: The morphology of experimentally produced charcoal distinguishes fuel types in the Arctic tundra, The Holocene, 30(7), 1091–1096, https://doi.org/10.1177/0959683620908629, 2020.

Peters, M. E. and Higuera, P. E.: Quantifying the source area of macroscopic charcoal with a particle dispersal
900 model, Quat. Res., 67(2), 304–310, https://doi.org/10.1016/j.yqres.2006.10.004, 2007.

Philben, M., Kaiser, K. and Benner, R.: Biochemical evidence for minimal vegetation change in peatlands of the West Siberian Lowland during the Medieval Climate Anomaly and Little Ice Age, J. Geophys. Res. Biogeosciences, 119(5), 808–825, https://doi.org/10.1002/2013JG002396, 2014.

Philippsen, B.: The freshwater reservoir effect in radiocarbon dating, Herit. Sci., 1–24,
905 https://doi.org/10.1186/2050-7445-1-24, 2013.

Pisaric, M. F. J.: Long-distance transport of terrestrial plant material by convection resulting from forest fires, J. Paleolimnol., 28(3), 349–354, https://doi.org/10.1023/A:1021630017078, 2002.

Pitulko, V. V., Nikolsky, P. A., Girya, E. Y., Basilyan, A. E., Tumskoy, V. E., Koulakov, S. A., Astakhov, S. N., Pavlova, E. Y. and Anisimov, M. A.: The Yana RHS site: humans in the Arctic before the Last Glacial Maximum,
910 Science, 303(5654), 52–56, https://doi.org/10.1126/science.1085219, 2004.

Power, M. J., Marlon, J., Ortiz, N., Bartlein, P. J., Harrison, S. P., Mayle, F. E., Ballouche, A., Bradshaw, R. H. W., Carcaillet, C., Cordova, C., Mooney, S., Moreno, P. I., Prentice, I. C., Thonicke, K., Tinner, W., Whitlock, C., Zhang, Y., Zhao, Y., Ali, A. A., Anderson, R. S., Beer, R., Behling, H., Briles, C., Brown, K. J., Brunelle, A., Bush, M., Camill, P., Chu, G. Q., Clark, J., Colombaroli, D., Connor, S., Finsinger, W., Foster, D., Frechette, J.,
915 Hallett, D. J., Higuera, P., Hope, G., Horn, S., Inoue, J., Kaltenrieder, P., Kennedy, L., Kong, Z. C., Larsen, C., Long, C. J., Lynch, J., Lynch, E. A., McGlone, M., Meeks, S., Mensing, S., Meyer, G., Minckley, T., Mohr, J., Nelson, D. M., New, J., Newnham, R., Noti, R., Oswald, W., Pierce, J., Richard, P. J. H., Rowe, C., Turney, C., Urrego-Sanchez, D. H., Umbanhowar, C., Vandergoes, M., Vanniere, B., Vescovi, E., Walsh, M., Wang, X., Williams, N., Wilmshurst, J. and Zhang, J. H.: Changes in fire regimes since the Last Glacial Maximum: an
920 assessment based on a global synthesis and analysis of charcoal data, Clim Dyn, 30, 887–907, https://doi.org/10.1007/s00382-007-0334-x, 2008.

Power, M. J., Marlon, J. R., Bartlein, P. J. and Harrison, S. P.: Fire history and the Global Charcoal Database: A new tool for hypothesis testing and data exploration, Palaeogeogr. Palaeoclimatol. Palaeoecol., 291(1), 52–59, https://doi.org/10.1016/j.palaeo.2009.09.014, 2010.

925 Pyne, S. J.: Wild hearth. A prolegomenon to the cultural fire history of Northern Eurasia, in Fire in Ecosystems of Boreal Eurasia, edited by J. G. Goldammer and V. V. Furyaev, pp. 21–44, Springer Netherlands, Dordrecht, 1996.

R Core Team: R: A language and environment for statistical computing, R Foundation for Statistical Computing, Vienna, Austria, available at https://www.R-project.org/ (last access: 21 October 2020), 2020

Reimer, P. J., Austin, W. E. N., Bard, E., Bayliss, A., Blackwell, P. G., Ramsey, C. B., Butzin, M., Cheng, H.,
930 Edwards, R. L., Friedrich, M., Grootes, P. M., Guilderson, T. P., Hajdas, I., Heaton, T. J., Hogg, A. G., Hughen, K. A., Kromer, B., Manning, S. W., Muscheler, R., Palmer, J. G., Pearson, C., Plicht, J. van der, Reimer, R. W., Richards, D. A., Scott, E. M., Southon, J. R., Turney, C. S. M., Wacker, L., Adolphi, F., Büntgen, U., Capano, M., Fahrni, S. M., Fogtmann-Schulz, A., Friedrich, R., Köhler, P., Kudsk, S., Miyake, F., Olsen, J., Reinig, F., Sakamoto, M., Sookdeo, A. and Talamo, S.: The IntCal20 Northern Hemisphere radiocarbon age calibration curve
935 (0–55 cal kBP), Radiocarbon, 62(4), 725–757, https://doi.org/10.1017/RDC.2020.41, 2020.

Remy, C. C., Fouquemberg, C., Asselin, H., Andrieux, B., Magnan, G., Brossier, B., Grondin, P., Bergeron, Y., Talon, B., Girardin, M. P., Blarquez, O., Bajolle, L. and Ali, A. A.: Guidelines for the use and interpretation of palaeofire reconstructions based on various archives and proxies, Quat. Sci. Rev., 193, 312–322, https://doi.org/10.1016/j.quascirev.2018.06.010, 2018.

940 Revelle, W.: psych: Procedures for Personality and Psychological Research, Northwestern University, Evanston, Illinois, USA, available at https://CRAN.R-project.org/package=psych Version = 2.0.7 (last access 21 October 2020), 2020

Rogers, B. M., Soja, A. J., Goulden, M. L. and Randerson, J. T.: Influence of tree species on continental differences
945 in boreal fires and climate feedbacks, Nat. Geosci., 8(3), 228–234, https://doi.org/10.1038/ngeo2352, 2015.

Russian Institute of Hydrometeorological Information: World Data Center, available at http://meteo.ru/english/climate/temp.php (last access: 21 October 2020), 2020

Scheffer, M., Hirota, M., Holmgren, M., Nes, E. H. V. and Chapin, F. S.: Thresholds for boreal biome transitions,
950 Proc. Natl. Acad. Sci., 109(52), 21384–21389, https://doi.org/10.1073/pnas.1219844110, 2012.

Schepaschenko, D. G., Shvidenko, A. Z. and Shalaev, V. S.: Biological Productivity and Carbon Budget of Larch Forests of Northern-East Russia, Moscow State Forest University, Moscow, 2008

Séjourné, A., Costard, F., Fedorov, A., Gargani, J., Skorve, J., Massé, M. and Mège, D.: Evolution of the banks of
955 thermokarst lakes in Central Yakutia (Central Siberia) due to retrogressive thaw slump activity controlled by insolation, Geomorphology, 241, 31–40, https://doi.org/10.1016/j.geomorph.2015.03.033, 2015.

Sofronov, M. A. and Volokitina, A. V.: Wildfire ecology in continuous permafrost zone, in: Permafrost Ecosystems: Siberian Larch Forests, edited by A. Osawa, O. A. Zyryanova, Y. Matsuura, T. Kajimoto and R. W. Wein, pp. 59–82, https://doi.org/10.1007/978-1-4020-9693-8_4, Springer Science+Business Media B.V.,
960 Dordrecht, 2010

Sofronov, M. A., Volokitina, A. V. and Shvidenko, A. Z.: Wildland fires in the north of Central Siberia, Commonwealth Forestry Rev., 77, 211–218, 1998

Tinner, W., Hofstetter, S., Zeugin, F., Conedera, M., Wohlgemuth, T., Zimmermann, L. and Zweifel, R.: Long-distance transport of macroscopic charcoal by an intensive crown fire in the Swiss Alps - implications for fire history reconstruction, The Holocene, 16(2), 287–292, https://doi.org/10.1191/0959683606hl925rr, 2006.

Vaganov, E. A. and Arbatskaya, M. K.: Climate history and wildfire frequency in the central part of Krasnoyarsky Krai. Climatic conditions in growing season and seasonal wildfires distribution, Siberian J. Ecol., 3, 9–18

van den Boogaart, K. G., Tolosana-Delgado, R. and Bren, M.: compositions: Compositional Data Analysis. R package version 2.0-0, available at https://CRAN.R-project.org/package=compositions (last access 21 October 2020), 2020

Vyse, S. A., Herzschuh, U., Andreev, A. A., Pestryakova, L. A., Diekmann, B., Armitage, S. J. and Biskaborn, B. K.: Geochemical and sedimentological responses of arctic glacial Lake Ilirney, Chukotka (Far East Russia) to palaeoenvironmental change since ~51.8 ka BP, Quat. Sci. Rev., 247, 106607, https://doi.org/10.1016/j.quascirev.2020.106607, 2020.

Waito, J., Girardin, M. P., Tardif, J. C., Conciatori, F., Bergeron, Y. and Ali, A. A.: Recent fire activity in the boreal eastern interior of North America is below that of the past 2000 yr, Ecosphere, 9(6), e02287, https://doi.org/10.1002/ecs2.2287, 2018.

Walker, X. J., Baltzer, J. L., Cumming, S. G., Day, N. J., Ebert, C., Goetz, S., Johnstone, J. F., Potter, S., Rogers, B. M., Schuur, E. A. G., Turetsky, M. R. and Mack, M. C.: Increasing wildfires threaten historic carbon sink of boreal forest soils, Nature, 572(7770), 520–523, https://doi.org/10.1038/s41586-019-1474-y, 2019.

Wallenius, T.: Major decline in fires in coniferous forests - Reconstructing the phenomenon and seeking for the cause, Silva Fennica, 45(1), 139–155, https://doi.org/10.14214/sf.36, 2011.

Wallenius, T., Larjavaara, M., Heikkinen, J. and Shibistova, O.: Declining fires in *Larix*-dominated forests in northern Irkutsk district, Int. J. Wildland Fire, 20(2), 248–254, https://doi.org/10.1071/WF10020, 2011.

Wang, S. and Hausfather, Z.: ESD Reviews: mechanisms, evidence, and impacts of climate tipping elements, Earth Syst. Dyn. Discuss., 1–93, https://doi.org/https://doi.org/10.5194/esd-2020-16, 2020.

Ward, D. E. and Hardy, C. C.: Smoke emissions from wildland fires, Environ. Int., 17, 117–134, 1991.

West, J. J. and Plug, L. J.: Time-dependent morphology of thaw lakes and taliks in deep and shallow ground ice, J. Geophys. Res. Earth Surf., 113, F01009, https://doi.org/10.1029/2006JF000696, 2008.

Whitlock, C. and Anderson, R. S.: Fire history reconstructions based on sediment records from lakes and wetlands, in Fire and Climatic Change in Temperate Ecosystems of the Western Americas, edited by T. T. Veblen, W. L. Baker, G. Montenegro, and T. W. Swetnam, pp. 3–31, Springer, New York, NY., 2003.

Whitlock, C. and Larsen, C.: Charcoal as a fire proxy, in Tracking Environmental Change Using Lake Sediments vol. 3: Terrestrial, Algal, and Siliceous Indicators, edited by J. P. Smol, H. J. B. Birks, and W. M. Last, pp. 75–97, Springer Netherlands, Dordrecht., 2001.

Wirth, C.: Fire regime and tree diversity in boreal forests: implications for the carbon cycle, in Forest Diversity and Function: Temperate and Boreal Systems, edited by M. Scherer-Lorenzen, C. Körner, and E.-D. Schulze, pp. 309–344, Springer, Berlin, Heidelberg., 2005.

1000   Wohlfarth, B., Skog, G., Possnert, G. and Holmquist, B.: Pitfalls in the AMS radiocarbon-dating of terrestrial macrofossils, J. Quat. Sci., 13(2), 137–145, 1998.

Woodward, C. and Haines, H. A.: Unprecedented long-distance transport of macroscopic charcoal from a large, intense forest fire in eastern Australia: Implications for fire history reconstruction, The Holocene, 30(7), 947–952, https://doi.org/10.1177/0959683620908664, 2020.

1005   Wu, B. and Wang, J.: Winter Arctic Oscillation, Siberian High and East Asian Winter Monsoon, Geophys. Res. Lett., 29(19), 1897, https://doi.org/10.1029/2002GL015373, 2002.